Chem Soc Rev

This article was published as part of the

Hybrid materials themed issue

Guest editors Clément Sanchez, Kenneth J. Shea and Susumu Kitagawa

Please take a look at the issue 2 2011 table of contents to access other reviews in this themed issue

Controlled pore formation in organotrialkoxysilane-derived hybrids: from aerogels to hierarchically porous monoliths†

Kazuyoshi Kanamori and Kazuki Nakanishi*

Received 6th August 2010
DOI: 10.1039/c0cs00068j

Porous polysilsesquioxane gels derived from sol–gel systems based on trifunctional silanes are reviewed. Although it is well known that trifunctional silanes possess inherent difficulties in forming homogeneous gels, increasing attention is being paid on these precursors and resultant porous polysilsesquioxanes because of hydrophobicity, functionality, and versatile mechanical properties. Much effort has been made to overcome the difficulties for homogeneous gelation, and a number of excellent porous materials with various pore properties have been explored. In this *critical review*, we put special emphasis on the formation of a well-defined macroporous structure by making use of phase separation, which in turn is a serious problem in obtaining homogeneous gels though. Porous polysilsesquioxane monoliths with the hierarchical structure and transparent aerogels with high mechanical durability are particularly highlighted (169 references).

1. Introduction

From the very beginning of sol–gel history, silica has been the central core of researchers' interest. The first reason is that the formation of silica networks from tetraalkoxysilanes with moderate reactivity is facile and controllable by varying the synthesis conditions such as pH, temperature, and additives.[1] Other reasons can be found in the ease of incorporation of organic molecules or moiety, polymers, and biomolecules or cells owing to the liquid-phase reactions that can be processed at low temperatures. Enormous achievements including functionalization and enhancement of mechanical properties by hybridization of silica-based networks (as well as other metalloxane networks) with above-mentioned incorporates are reviewed in the literature.[2–10]

One of the representative ways to hybridize siloxane networks with organic (functional) groups is to use organotrialkoxysilanes, which will be focused in this review, or bis(trialkoxysilyl)organometallic compounds.[11,12] The organic (functional) groups are directly attached to silicon in these silanes and usually do not react in the course of the hydrolysis and condensation reactions. The typical examples include, as described in greater detail below, trialkoxysilanes with substituent groups such as methyl, ethyl, vinyl, allyl, phenyl, aminopropyl, mercaptopropyl, methacryloxypropyl, glycidoxypropyl, and many others. Bis(trialkoxysilyl)organometallic compounds involve those bridged with methylene, ethylene, phenylene groups, *etc*. While the organic groups are incorporated as dangling groups in the networks derived from trialkoxysilanes, the organic moiety in the bridged alkoxysilanes-derived networks

Department of Chemistry, Graduate School of Science, Kyoto University, Kitashirakawa, Sakyo-ku, Kyoto 606-8502, Japan. E-mail: kanamori@kuchem.kyoto-u.ac.jp, kazuki@kuchem.kyoto-u.ac.jp; Fax: +81-75-753-7673, +81-75-753-2925; Tel: +81-75-753-7673, +81-75-753-2925

† Part of the themed issue on hybrid materials.

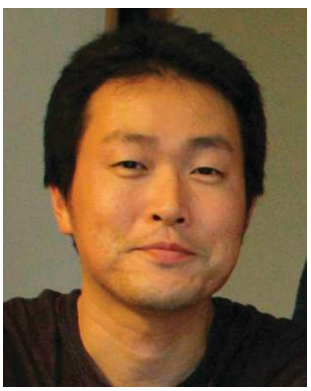

Kazuyoshi Kanamori

Kazuyoshi Kanamori received his Bachelor (2000), Master (2002), and Doctor of Engineering (2005) from Kyoto University. He worked as a postdoctoral fellow of JSPS from 2005 to 2007. He is currently an Assistant Professor at Department of Chemistry, Graduate School of Science, Kyoto University. His research interest is based on synthesis, characterization, and application of porous materials prepared via liquid-phase processes such as the sol–gel method and living polymerization in polymer chemistry. Porous materials composed of inorganic oxides, organic–inorganic hybrids, organic cross-linked polymers, and carbons are his particular concerns.

Kazuki Nakanishi

Kazuki Nakanishi is an Associate Professor of Department of Chemistry, Graduate School of Science, Kyoto University. He became interested in the competitive processes between phase separation and sol–gel transition in 1986 when he joined Department of Material Chemistry, Graduate School of Engineering, Kyoto University. His research has been focused on the integrated design of hierarchically porous materials in various chemical compositions such as pure and complex oxide ceramics, organic–inorganic hybrids and colloidal systems. Monolithic silica columns for HPLC is one of his major inventions.

 This journal is © The Royal Society of Chemistry 2011

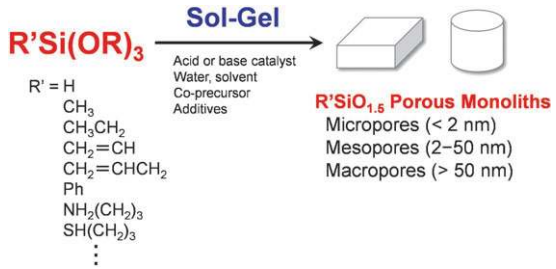

Fig. 1 Porous organic–inorganic hybrid materials obtained from sol–gel chemistry of organotrialkoxysilanes. Monolithic materials are particularly reviewed in this article.

connects two neighboring silicons. Besides, chemistry of the network formation is considerably different between these precursors though the chemical formulae of the precursors and the resultant materials are similar to each other.[13,14] Surface and mechanical properties are therefore significantly different between these two types of hybrids as discussed later.

In this review, we specially focus on the properties and pore formations in organic–inorganic hybrid siloxane networks derived from organotrialkoxysilanes sol–gel systems (Fig. 1). Monolithic porous materials are particularly emphasized. Various porous hybrid materials embedded with micropores (pore size <2 nm), mesopores (2–50 nm), and macropores (>50 nm), including aerogels and hierarchically porous materials with more than two discrete levels of pores, are reviewed.

2. A brief note on sol–gel chemistry of trifunctional silanes

The condensation products of trifunctional silanes are called silsesquioxanes[15] since the products contain $RSiO_{1.5}$ formula where R is a substituent unit. The Latin prefix "sesqui" means "1.5" and silsesquioxane stands for compounds containing silicon and oxygen with O/Si atomic ratio of 1.5. The word "*poly*silsesquioxane" should be reserved for polymers or networks consisting of $RSiO_{1.5}$, and for oligomers such as polyhedral oligomeric silsesquioxanes (POSS), one should not use the word "*poly*silsesquioxane". Condensates from bridged alkoxysilanes such as α,ω-bis(trimethoxysilyl)alkanes are also called as silsesquioxanes because O/Si atomic ratio is 1.5 as well. Here we focus on the polysilsesquioxanes obtained from trifunctional silanes. Fig. 2 represents the several well-known structures derived from trifunctional silanes. Formation of random networks (a) can lead to homogeneous gelation and competitive cyclization reactions can result in ladder (b) and (partial) cage structures (c and d) as described later. These (partially) closed structures do not contribute homogeneous gelation but result in crystalline precipitates. The ladder structure was suggested by Brown *et al.* for the first time with insufficient evidence.[16] However, there are some reports describing that "true" ladder structures can be obtained by a controlled reaction of cyclic silanol compounds or oxidation of polysilanes.[17–19]

The hydrolysis and polycondensation reactions in sol–gel systems of trialkoxysilanes with an organic substituent are considerably affected by the type of substituent as well as by pH, temperature, *etc*. In particular, because of the inductive

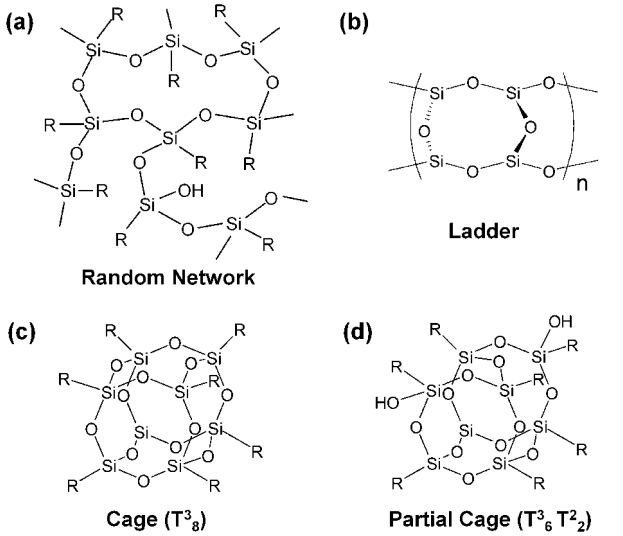

Fig. 2 Typical condensates derived from trifunctional silanes. (a) Random network structure that can lead to homogeneous gelation, (b) suggested ladder structure, (c) perfect cage structure of octamer, and (d) partial cage structure. Many other cage-like structures that form crystalline precipitates are also suggested.

effect and steric hindrance, reactivity of organotrialkoxysilanes is strongly dependent on the chemical nature of the substituent. Furthermore, phase separation in polar solvent gives a considerable effect on gelation of these precursors. Although phase separation can be advantageously used to control macropores in trialkoxysilane-derived gels as discussed later, this fact indicates that homogeneous gels with high transparency are hard to be obtained in the trialkoxysilane sol–gel systems, though controllability of homogeneous gelation is a basis of materials designing.

Reactions of a broad range of trimethoxy- and triethoxysilanes with organic substituents were studied by Loy *et al.*[13] They investigated (organo)trialkoxysilanes including alkyl (up to C_{18}), vinyl, phenyl, benzyl, *etc*., and reported that in any pH conditions, it is difficult to form homogeneous gels. For many organotrialkoxysilanes, only soluble resins, oils, or precipitates consisting of oligomers or low-molecular-weight polymers have been obtained as a result of inefficient hydrolysis and polycondensation reactions, cyclization, and phase separation of hydrophobic condensates in polar solvent. Especially in triethoxysilanes in acidic conditions, crystalline products presumably consisting of POSS are the dominant products. Trialkoxysilanes with small substituents such as hydrogen, methyl, and chloromethyl groups are more suitable to form gels with a good homogeneity. Compared to tetrafunctional precursors such as tetramethoxysilane (TMOS) and tetramethoxysilane (TEOS), alkyl-substituted trialkoxysilanes are reported to form gels (if possible) in a shorter time irrespective of the solution pH when reacted in the identical conditions to tetraalkoxysilanes; one must be careful because both tetrafunctional and trifunctional silanes are reacted with the same molar ratio of water/Si (r) = 1.5. Although this is stoichiometric for trifunctional monomers, it is below the stoichiometry for tetrafunctional monomers. Besides, phase separation in trifunctional systems accelerates gelation because

monomers and oligomers are concentrated in one of the phases after the onset of phase separation and more effectively undergo condensation with nearer neighboring species. Hence, in fact, the reaction rate is strongly dependent on various factors including monomer concentration, solution pH, r, phase separation, and steric hindrance. Differences in reactivity in trialkoxysilanes and tetraalkoxysilanes are discussed later from the viewpoint of reaction mechanisms.

The reactivity based on the inductive effect of trialkoxysilanes can be quantitatively evaluated using the "partial charge model" proposed by Livage and Henry.[20] According to this model, the partial charge (δ_i) of an element i in a molecule can be calculated by taking electronegativity (χ_i) in a neutral state of all elements in the molecule. The mean electronegativity $\bar{\chi}$ of the molecule is calculated as

$$\bar{\chi} = \frac{\sum_i \sqrt{\chi_i} + 1.36z}{\sum_i (1/\chi_i)}, \quad (1)$$

where z represents the electric charge for charged species such as ions. The partial charge on an element in the molecule is then given by

$$\delta_i = \frac{\bar{\chi} - \chi_i}{1.36\sqrt{\chi_i}}. \quad (2)$$

After Livage *et al.*, if we apply electronegativity values $\chi_C = 2.50$, $\chi_H = 2.1$, $\chi_O = 3.50$, and $\chi_{Si} = 1.74$,[21] we obtain the partial charge on oxygen and silicon in some alkoxysilanes as listed in Table 1.

It is also helpful to introduce group electronegativity[22] mainly used in organic chemistry. The values of various group electronegativity are calculated by counting the number of valence electrons n^* on the central atom of a radical $^\bullet$AB as

$$n^* = (N - p) + \frac{2m\chi_B}{\chi_A + \chi_B} - \frac{s\chi_A}{\chi_A + \chi_B} \quad (3)$$

where N and p are the numbers of valence electrons on the free atom A and of valence electrons supplied by B when forming the A–B bond, respectively. The number of bonds between A and B, and the number of resonance contributions from A^-B^+ are included as m and s. Group electronegativity χ^g is then calculated as

$$\chi^g = 0.31\left(\frac{n^* + 1}{r_A}\right) + 0.50 \quad (4)$$

with r_A being the covalent radius of atom A in the radical $^\bullet$AB. Some of the χ^g values that are useful in sol–gel chemistry of alkoxysilanes are listed in Table 2.

Table 1 Partial charge values δ_i of various silanes calculated by the partial charge model

	$Si(OR)_4$	$CH_3Si(OR)_3$	$C_2H_5Si(OR)_3$
δ_O values			
R = CH_3	−0.44	−0.46	−0.47
R = C_2H_5	−0.46	−0.47	−0.48
R = C_3H_7	−0.47	−0.48	−0.48
δ_{Si} values			
R = CH_3	+0.35	+0.33	+0.32
R = C_2H_5	+0.32	+0.31	+0.31
R = C_3H_7	+0.31	+0.30	+0.30

Table 2 Group electronegativity χ^g values relevant to silanes-based sol–gel chemistry[a]

Group	χ^g	Group	χ^g
$-CH_3$	2.47	–H	2.62
$-C_2H_5$	2.48	–OH[b]	3.49
$-C_3H_7$	2.48	$-OCH_3$	3.54
$-C_6H_5$ (–Ph)	2.72	$-OC_2H_5$	3.54
$-CH=CH_2$	2.79	$-SiCl_3$	2.10
$-NH_2$	2.99	Si[c]	1.84

[a] Calculated using Gordy's electronegativity. [b] Hydroxide groups are believed to be more electronegative and withdraw more electrons than alkoxy groups presumably due to the solvation effects in polar solvent. [c] Gordy's electronegativity for neutral Si.

In acidic media, since the attack of proton onto the oxygen in the alkoxy group is the rate-determining step of hydrolysis, the more electronegative charge (larger $|\delta_O|$, $\delta_O < 0$) on alkoxide oxygen allows faster hydrolysis. Although alkyl groups are known as electron donating groups in carbon-based organic chemistry, they to some extent withdraw electrons from silicon because electronegativity of alkyl groups is larger than silicon as shown in Table 2. By comparing with tetraalkoxysilanes, however, oxygen in alkyltrialkoxysilanes has higher electron density because the electron-withdrawing ability of alkyl groups is weaker than alkoxy groups. For this reason, alkyltrialkoxysilanes and relevant trifunctional silanes substituted with such as phenyl and vinyl groups are therefore more susceptible to hydrolysis than tetraalkoxysilanes in an acid-catalyzed system. However, one must be careful about the steric hindrance given by the substituted groups; bulky substituents such as long and branched alkyl chains and those containing aromatic groups tend to retard hydrolysis because the nucleophilic attack of water molecule to the central silicon, which is also an important step for hydrolysis, becomes increasingly difficult. In practice, while small substituent like hydrogen and methyl, ethyl and vinyl groups contribute to more rapid hydrolysis and condensation compared to tetraalkoxysilanes, large aliphatic and aromatic substituents considerably retard the reactions.

In basic media, conversely, substitution by less electron withdrawing groups compared to alkoxy groups makes alkoxides less reactive in hydrolysis and condensation because the partial charge on the central silicon becomes less positive (smaller $|\delta_{Si}|$, $\delta_{Si} > 0$), which fact makes the silicon less sensitive to the nucleophilic attack of HO^- and SiO^-. Compared to the tetrafunctional monomers with the same type of alkoxy group, trifunctional monomers with less-electron withdrawing groups (smaller χ^g) are more reactive in acid-catalyzed hydrolysis, but less reactive in base-catalyzed hydrolysis. One should again keep in mind that steric hindrance largely affects the reactivity.

Bridged alkoxysilanes systems also follow the similar inductive effects, but steric effects are believed to be small.[14] Moreover, since the precursors are regarded as hexafunctional, there is lower probability to form *inter*-molecular cyclic species. Instead, *intra*-molecular cyclization occurs in especially those with the C_1–C_4 alkylene bridges and homogeneous gelation is strongly hindered by the preferential formation of thermodynamically stable cyclic species.[23,24] Compared to

This journal is © The Royal Society of Chemistry 2011

organotrialkoxysilanes system, the homogeneous gelation in bridged alkoxysilane systems is considerably easier. It is therefore advantageous especially for the purpose of preparing aerogels with high porosity because the bridged precursors readily cause gelation even in dilute conditions. However, owing to rich surface chemistry and mechanical properties, organotrialkoxysilanes-derived polysilsesquioxane gels attract attention from various fields as described below.

It is also well-known that trifunctional silanes form crystalline POSS[15,25–27] represented by the cage structures as shown in Fig. 2(c) and (d) (there are many other cage structures suggested) as a result of hydrolysis and condensation. The typical POSS with an octahedral cage structure T^3_8 (in the notation of T^a_b, "T" stands for the maximum three siloxane bonds for each silicon, "*a*" is the actual number of siloxane bonds on each silicon, and "*b*" is the number of silicons in the unit) is synthesized from trichlorosilanes or trialkoxysilanes with excess water and organic solvent such as acetone, alcohol, toluene, and THF. Since silanols are highly reactive and therefore the POSS formation and random networking (Fig. 2(a)) are competitive, generally the POSS yield is not very high.[28] Nevertheless, since POSS is an important building block for improving properties such as solvent resistivity, mechanical strength and thermal stability, POSS is widely utilized to modify organic polymers through functionalization by hydrosilylation, *etc*.[29] Porous materials based on POSS or double-four-ring (D4R), which is another nomenclature for 8-membered POSS, are also the area of interest because of the possibility for new nano-building units.[30–34]

3. Various porous materials derived from trifunctional silanes

Porous hybrids with various functionality and thermal and mechanical properties are technologically important materials especially in the field of adsorption, catalysis and separation. In any applications, pore properties such as pore size, pore volume, surface area and pore geometry as well as shapes of materials (monoliths, films and particles) should be versatilely controlled to meet given requirements. Moreover, organic functional groups should be kept unchanged throughout the preparation process and in the used environments. As is well-known, the sol–gel process is suitable for tailoring hybrid functional porous materials owing to the controllable liquid-phase process that can be conducted at low temperatures.

For the pore formation through a controlled reaction of trifunctional silanes, alkoxysilanes (not chlorosilanes) are often employed due to the moderate reactivity and chemical stability. Trialkoxysilanes with small substituents such as hydrogen, methyl, ethyl and vinyl groups have been favored to tailor porous gels, though there are not many reports on trialkoxysilanes-derived porous materials because of the aforementioned difficulties in forming gels. We will later focus on some examples for these systems.

In other cases, co-gelation with tetrafunctional or bridged alkoxysilanes has been extensively investigated in order to satisfy both the inclusion of the relatively large functional substituents and homogeneous gelation. In this case, one should keep in mind that different reactivities of organotrialkoxysilane and tetraalkoxysilane or bridged alkoxysilane often cause serious heterogeneity in a way that the more reactive component forms siloxane networks in a shorter time, followed by the retarded condensation of the less-reactive one on the preformed networks. Hydrolysis and condensation of the less-reactive component should be performed to some extent in advance of the addition of the more-reactive one. Further, the desired pore structure may not be obtained if too much organotrialkoxysilane monomer is used. This is due to the decrease in cross-linking density, and gels would be more soft and friable resulting in the collapse of pores during drying. In the case of preparing ordered mesoporous materials as schematically shown in Fig. 3(a), since the organotrialkoxysilanes weaken the attractive interaction between condensates and surfactant, which is required for structure-directing, the pore periodicity tends to be lost as mentioned later. For an exception, the recent technology using amino-functionalized trialkoxysilanes as the co-structure directing agents (CSDA) is particularly unique and important for chiral ordered mesoporous silicas.[35–39] Electrostatic interaction between chiral surfactant and quaternized amino groups in organotrialkoxysilane plays a central role in this instance.

The successfully-obtained functionalized porous hybrids with ordered or disordered porosity potentially open up applications to solid acid catalysts,[40,41] ion-exchanging materials,[42,43] adsorbents for heavy metals,[44–46] and molecular imprinting materials,[47,48] exploiting surface functionality and pore characteristics.

As a different methodology, since surface functionalization of preformed porous materials[49–54] (such as mesoporous silicas MCM-41 and SBA-15) is facile and easy to control as shown in Fig. 3(b), much research on surface-functionalized silicas has been conducted for applications to catalyst supports,[55–62] heavy-metal or contaminant removal,[63–65] separation media,[66–69] optical and photonic devices,[70–72] *etc*. Amino- and mercapto-functionalized mesoporous silicas are most widely studied because of the reactivity of amino and thiol functional groups. Recent reviews on both the co-gelation method and surface modification of mesoporous silicas are found in the literature.[73–76] In addition, some commercially available products of functional (porous) hybrids are also reviewed.[77,78]

A sophisticated approach to tailor ordered mesoporous materials only from trialkoxysilanes is demonstrated and reviewed by Shimojima and Kuroda.[79,80] They hydrolyzed amphiphilic alkyltrialkoxysilanes (with C_{12}–C_{18}) in acidic media to obtain crystalline alkylsilanetriols and the subsequent drying step allows solid-state polycondensation to yield mesostructured hybrids with the lamellar symmetry (Fig. 4). Films with submicron thicknesses are also successfully prepared using this system. Moreover, by enlarging the alkoxysilane moiety into large siloxane head groups by controlled co-condensation with TMOS, they obtained mesoporous hybrids with different symmetries such as 2-D hexagonal and 2-D monoclinic. The surfactant-like amphiphilic property of alkyltrialkoxysilanes is proven to be useful for tailoring mesoporous hybrids.

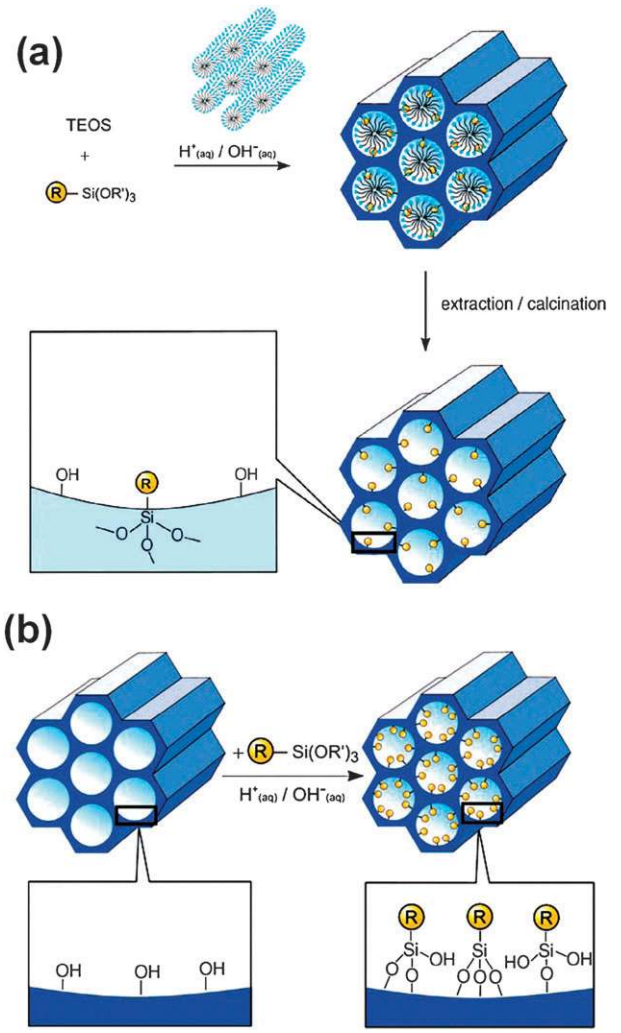

Fig. 3 Formations of functionalized mesoporous silicas. (a) Co-gelation of organotrialkoxysilane and tetraalkoxysilane directly forms functionalized mesoporous silica. (b) Surface modification process imparts functional groups on the surface of preformed mesoporous silica. From ref. 73 (Copyright Wiley-VCH Verlag GmbH & Co. KGaA. Reproduced with permission).

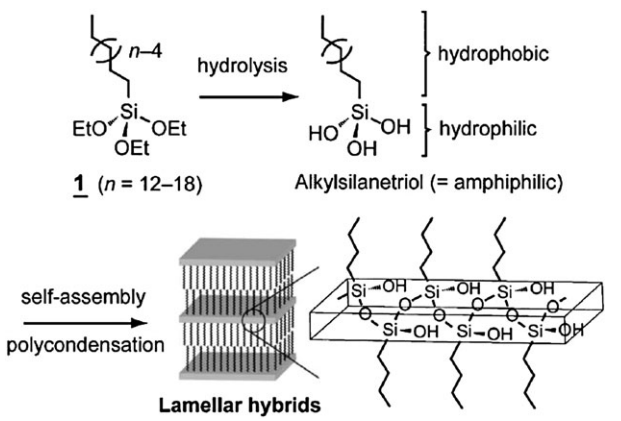

Fig. 4 Lamellar hybrids obtained from amphiphilic alkyltrialkoxysilanes with different chain lengths (**1**). From ref. 80.

For the preparation of monolithic macroporous materials with much larger pores (submicrons and microns), we have utilized trifunctional monomers such as methyltrimethoxysilane (MTMS)[81,82] and vinyltrimethoxysilane (VTMS).[83] In these alkoxides with hydrophobic groups, phase separation (spinodal decomposition) is induced in low-molecular-weight polar solvent and well-defined macropores are regulated in the course of sol–gel transition. The relative timing of phase separation and gelation determines the macroporous structure from "no distinct macropores", "bicontinuous", "particle aggregates", and to "macroscopic double phase" with increasing phase separation tendency.[84,85] In particular, bicontinuous structure, in which both gelled skeletons and macropores are co-continuous and forming a three-dimensional (3-D) sponge-like porous structure, is important morphology because of its well-defined geometry and controllability in pore characteristics such as size and volume. In some cases, morphology with isolated pores can be seen and is analogous to bicontinuous structure but connectivity of pores is lost due to the lower volume fraction of pores. With carefully controlling molar ratios of solvent and water relative to silicon (typically $r \approx 2.0$), monolithic gels are obtained in strongly acidic conditions. Enthalpic demixing of polar solvent and siloxane polymers, which become increasingly apolar in the progress of polycondensation, is the driving force of phase separation. Fig. 5 represents the starting composition–morphology relationship in both MTMS (left) and VTMS (center) systems containing formamide (FA) as the polar solvent and 1 M aqueous nitric acid (NAaq) as the catalyst. In the MTMS–FA–NAaq system, there are two possibilities to obtain well-defined macropores with bicontinuous structure; with smaller amount of water (NAaq) at around $r = 1.6$, MTMS is only partially hydrolyzed and phase separation tendency is high due to the presence of unreacted methoxy groups, and with higher amount of water at around $r = 2.5$, hydrolysis is almost complete and polymethylsilsesquioxane (PMSQ, $CH_3SiO_{1.5}$) gels with hydrophobic methyl groups phase-separate from the more polar solvent containing FA and water. With further increasing NAaq and FA, only gels with the macroscopic double phase are obtained, indicating a too high phase separation tendency. In the case of VTMS, bicontinuous structure forms only in the high concentration of VTMS (low concentrations of FA and NAaq) region due to the higher hydrophobicity of vinyl groups. Two compositional regions with different amounts of NAaq lead to bicontinuous structure with the same reason as in the MTMS system. In a co-gelation system with VTMS : TMOS = 8 : 2 in molar ratio (Fig. 5, right), bicontinuous structure is found to form in a broad compositional range as in the MTMS system. A moderate "average polarity" in the gel phase is important to broaden the moderate phase separation region with bicontinuous structure. Conversely, in the mixture system with VTMS : TMOS = 5 : 5, the compositional region of bicontinuous structure is small and the overall behavior resembles the TMOS–FA–NAaq system which phase-separates in the compositional region with limited amount of water ($r \approx 1.5$).[86,87] The same solvent-catalyst system containing allyltrimethoxysilane (ATMS), *i.e.* ATMS–FA–NAaq system, also shows the similar tendency with the VTMS system, but

This journal is © The Royal Society of Chemistry 2011

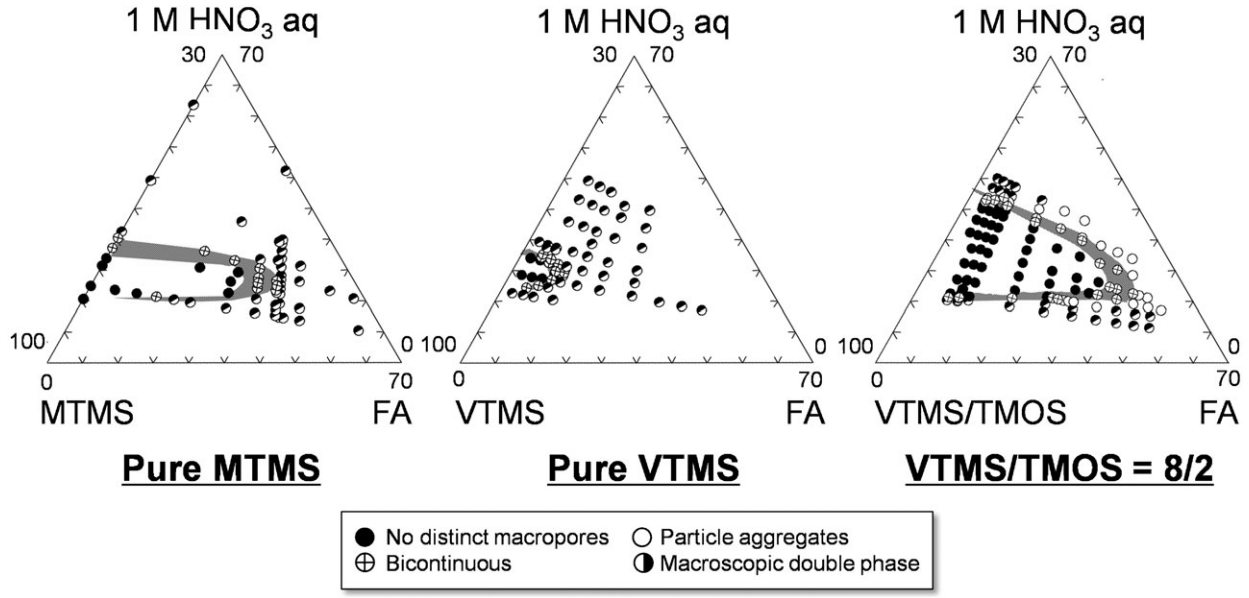

Fig. 5 Relationships between starting compositions and resultant morphology in three systems. From left to right, MTMS–FA–NAaq, VTMS–FA–NAaq, and VTMS/TMOS–FA–NAaq with VTMS/TMOS = 8/2 in molar ratio. All the starting compositions are in mass ratio.

requires more TMOS (such as ATMS : TMOS = 7 : 3) to extend the compositional region of bicontinuous structure because of the higher hydrophobicity of ATMS.

Fig. 6 shows the starting composition–morphology relationship in a system of MTMS–methanol (MeOH)–NAaq,[81,82] which is the modification of MTMS–FA–NAaq system. Since FA is hydrolyzed in a strongly acidic aqueous media into formic acid and ammonia, the solution pH increases to around 4.5, which is near the isoelectric point of alkylsilanetriol,[88] and gelation is considerably sluggish (~50 h). Moreover, the less-polar solvent methanol compared to FA reduces the too-strong repulsion between methylsiloxane polymers and the solvent. For these reasons, in MTMS–MeOH–NAaq system, macroporous structure is easier to be controlled with better reproducibility within a reasonable time scale (~3 h). Dong *et al.* also reported the preparation of macroporous MTMS-derived monolithic gels using the similar sol–gel systems.[89–91] Hydrolysis and condensation of MTMS in various pH conditions revealed that monolithic gels can be obtained only in a high pH (pH > 11) condition for the one-step method where both reactions proceed in the same pH condition throughout the process.[89] The solvent and water ratios were set as ethanol/MTMS = water/MTMS (r) = 4. For the acid/base two-step processes where hydrolysis and condensation undergo in different pH conditions, since the combination of effective hydrolysis in acidic conditions and vigorous condensation in basic conditions is established, monolithic gels are obtained in wider conditions. In this case, well-defined macroporous gels with bicontinuous structure are reported to form when the duration of acid-catalyzed hydrolysis is adequately controlled.[90]

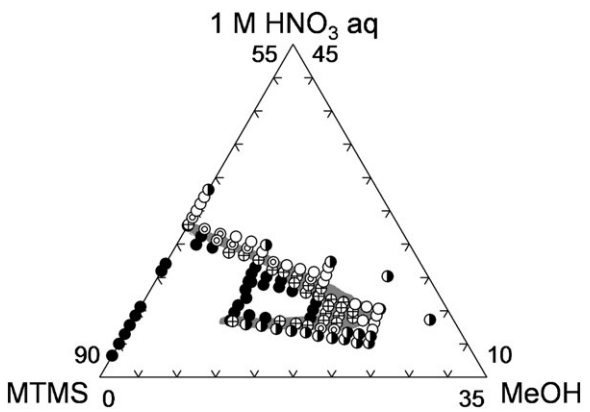

Fig. 6 Relationships between starting compositions (in mass %) and resultant morphology in MTMS–MeOH–NAaq system. Well-defined macropores are obtained in a broad compositional region and the moderate gelation time allows better structural controllability and reproducibility compared to MTMS–FA–NAaq system.

We also demonstrated that MTMS-derived macroporous films are obtained by the dip-coating method (Fig. 7).[92,93] Less-polar aprotic solvent *N*,*N*-dimethylformamide (DMF) was employed to attain moderate reaction and drying rates with starting compositions MTMS : DMF : water = 1 : 0.19 : 2.3 in molar ratio. The macroporous morphology is varied depending on the duration between the addition of MTMS and the onset of dipping a substrate (*i.e.* hydrolysis time). For shorter duration, since the MTMS-derived

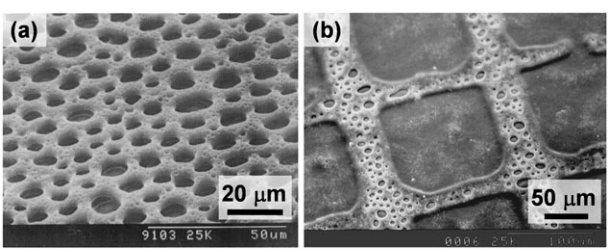

Fig. 7 Dip-coated macroporous PMSQ films derived from MTMS–DMF–NAaq solution. (a) A film on a polyester substrate and (b) that on a hydrophilic–hydrophobic patterned substrate.

oligomers and polymers are still small, it takes longer time for the evaporation-induced solidification on the substrate. As a result, the coarser structure is obtained in the case of shorter hydrolysis, and the finer structure forms in the case of longer hydrolysis. In addition, morphology is naturally dependent on the nature (hydrophilic or hydrophobic) of the substrate and it is expected that a patterning of macroporous films can be achieved by using a substrate with desired hydrophilic–hydrophobic patterns. In Fig. 7(b), a macroporous PMSQ film dip-coated on a patterned glass substrate is shown. The PMSQ gel is deposited on the hydrophilic silicate glass regions and no film is coated on the octadecylsilylated hydrophobic regions.

Since the film thickness available by the dip-coating process is only up to 10 μm, we employed another method in order to make thicker films and improve the 3-D porous structures. We prepared well-defined macroporous MTMS-derived thick films by intruding the starting sol in-between parallel plates,[81,82,94–96] which we call the "gap-filling method". By utilizing an aluminum substrate with hydrophilic silica layer and a carbon-coated hydrophobic silicate glass substrate, macroporous PMSQ films with 300 μm thickness were successfully obtained on the aluminum substrate as shown in Fig. 8.[97] The carbon-coated substrate can be readily removed because there forms virtually no chemical bonds between PMSQ and the substrate. Owing to the less-polarizable methyl-silicon bonds, the PMSQ films, which are often called as carbon-doped silica or SiCOH in the literature, are highly expected to have considerably low dielectric constant (low-k) required in recent microelectronics.[98–101] Porosity in these materials additionally contributes to decrease in the dielectric constant. The macroporous PMSQ films prepared in our research also showed low dielectric constant as k = 1.4–1.7 in a high AC frequency at 60 GHz characterized by the Fabry–Perot resonator method. Further elimination of polarizable groups such as silanol groups may lead to further decrease in the value of k. In addition, since a skin layer forms at the interface between PMSQ film and carbon-coated substrate as shown in Fig. 8(b), it was possible to design electronic circuits directly on the film. Although PMSQ is advantageous to reduce dielectric constant compared to silica, the pore formation using surfactant micelles, which is often applied to introduce porosity in silicate films, becomes difficult with increasing methyltrialkoxysilanes in co-gelation systems with tetraalkoxysilane.[102–105] This is attributed to the lower silanol density of PMSQ and being unable to interact through electrostatic attraction and hydrogen bonding with surfactant that is necessary to form mesopores.[106] Since our film-forming methods rely only on the phase separation behavior, broader applications for tailoring low-k materials are expected.

Another possibility of porous PMSQ materials has been proposed by investigating the applicability of the macroporous PMSQ gels to separation media used in high-performance liquid chromatography (HPLC).[81,107] It is revealed in Fig. 9 that MTMS-derived monolithic gels in a capillary (200 μm in diameter) can separate both polar and apolar molecules in the normal and reversed-phase modes, respectively, presumably because of the amphiphilic property of the PMSQ surface possessing both hydrophobic methyl and hydrophilic hydroxide (silanol) groups. A number of theoretical plates in the normal-phase mode, in particular, reach as high as 100 000 m^{-1}, and also we found that incorporation of nonionic surfactant alters the surface property so that the retention of analytes is altered.[81]

Differences in the surface property among siloxane-based gels prepared from various precursors can be evaluated from chromatographic separation tests. Fig. 10 illustrates the results of separations of toluene (t_0), 2,6-dinitrotoluene (retention time t_1) and 1,2-dinitrobenzene (t_2) in the normal-phase mode using three different columns derived from TMOS, 1,2-bis(trimethoxysilyl)ethane (BTME), and MTMS. Retention factors of 2,6-dinitrotoluene $k_1 = (t_1 - t_0)/t_0$ and that of 1,2-dinitrobenzene $k_2 = (t_2 - t_0)/t_0$ are calculated to give separation factors $\alpha = k_2/k_1$ for each column. If the surface is more polar or hydrophilic with higher surface silanol density, the most polar molecule 1,2-dinitrobenzene will be retained for longer duration, and the value of α becomes larger. Pure silica gel column shows the separation factor of 5.22 and PMSQ column shows the smaller value of 2.72 due to the existence of methyl groups and less surface silanol density. The BTME-derived column unexpectedly shows the higher value of α, which is even higher than pure silica, suggesting more surface silanol density and hydrophilicity at least in a length scale of a few nanometres. Note that since pores smaller than these sizes may not contribute to the separation, we cannot obtain any

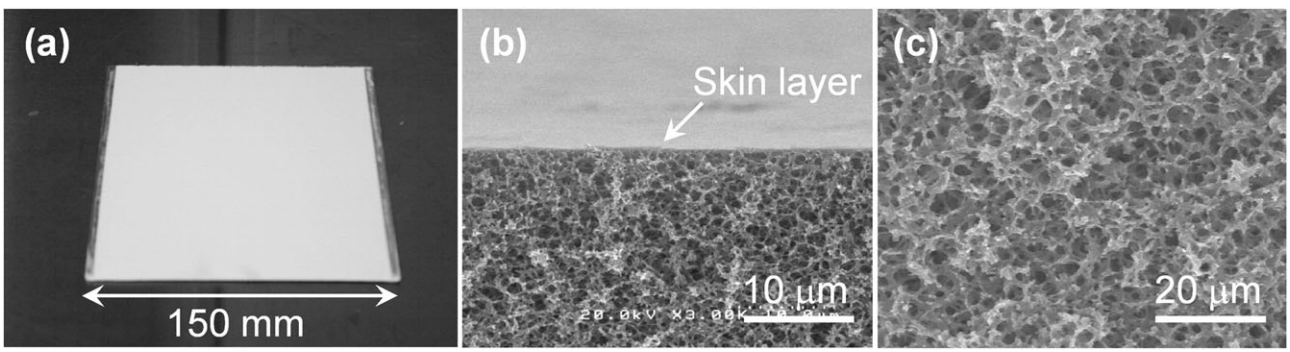

Fig. 8 An example of macroporous PMSQ thick film with thickness of 300 μm prepared by the gap-filling method. (a) The film area is as large as 150 × 150 mm^2. (b) The skin layer formed at the interface between the sol and carbon-coated glass substrate, and the layer can be used for mounting an electric circuit. (c) Macroporous structure in the cross-section of the film.

 This journal is © The Royal Society of Chemistry 2011

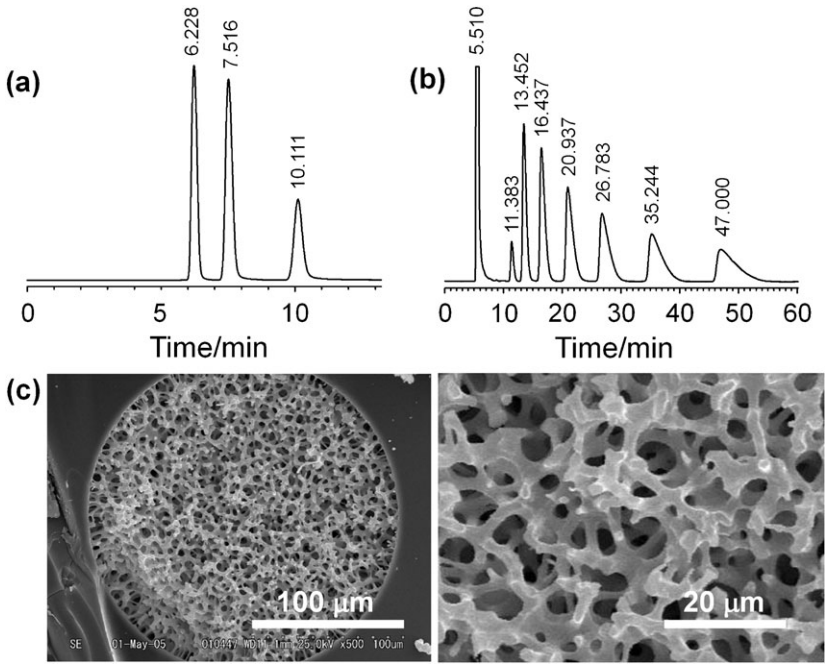

Fig. 9 (a) Normal-phase and (b) reversed-phase chromatograms obtained with a PMSQ capillary column with the macroporous structure exhibited in (c). The starting composition of the column is MTMS : MeOH : water = 1 : 1.2 : 2.0. Mobile phases in normal- and reversed-phase modes, are hexane/2-propanol (98/2 in volume) and methanol/water (80/20 in volume), respectively. Analyte samples in the normal-phase mode are toluene (t_0), 2,6-dinitrotoluene and 1,2-dinitrobenzene, and those in the reversed-phase are thiourea (t_0) and alkylbenzenes (C_nH_{2n+1})Ph (n = 0–6).

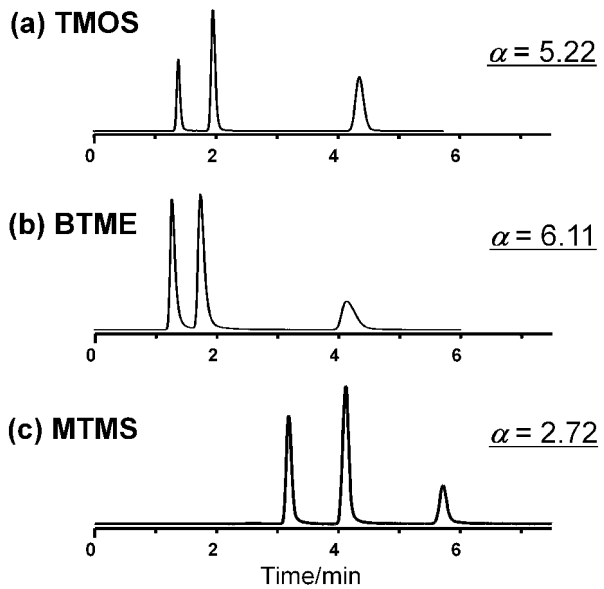

Fig. 10 Chromatographic separations of the polar molecules in the normal-phase mode by three different columns. The columns are derived from (a) tetramethoxysilane (TMOS), (b) 1,2-bis(trimethoxysilyl)ethane (BTME), and (c) methyltrimethoxysilane (MTMS). The separation factor α showing the extent of separation of the more polar molecules is introduced to evaluate the hydrophilic properties of each column. The BTME-derived column unexpectedly shows the highest α value, *i.e.* the highest hydrophilicity. See Fig. 9 (a) for conditions for separations.

information from chromatograms in a very short length scale. We therefore can anticipate that BTME forms relatively compact condensates with embedding hydrophobic bridging groups inside the networks and a large number of the surface silanol groups due to the hexafunctionality are exposed toward the solvent in the course of hydrolysis and polycondensation, resulting in a high hydrophilic property.

In many micro-sized applications such as to capillary HPLC and lab-on-a-chip, heterogeneity of the porous structure becomes a crucial problem. In small confined spaces such as a gap between 2-D parallel plates,[81,82,94–96] inside a 1-D capillary,[81,82,96] inside a open groove,[82,108,109] and inside 0-D macropores,[96,110] wetting phenomena,[111,112] in which one of the separated phases preferentially adsorb onto the existing surfaces, become to play a dominant role over the phase separation. In the case of MTMS–MeOH–NAaq system, after the onset of phase separation, the less-polar MTMS-derived gel-rich phase flows onto the microsurfaces and spreads there to form a film. The main driving force for this behavior is the lower interfacial energy of the gel-rich phase compared to the polar solvent-rich phase because silanol-consuming process lowers the cohesive interactions in the gel-rich phase during the gel-rich phase keeps fluidity (before the gel point). The microsurface must be wet by one of the phases with the lowest interfacial energy when the surface is forced to touch the phase-separating multi-phase liquid system, and the gel-rich phase usually preferentially wets the existing surface. This wetting process through a hydrodynamic flow[111] induces the heterogeneity particularly in the vicinity of the surface as shown in Fig. 11. In a fused silica capillary with a hydrophilic wall, pillars normal to the capillary walls are observed, through which pillars, wetting proceeded in a hydrodynamic way during phase separation. The wetting effect becomes much stronger with decreasing inner diameters of the capillaries as far as the starting composition

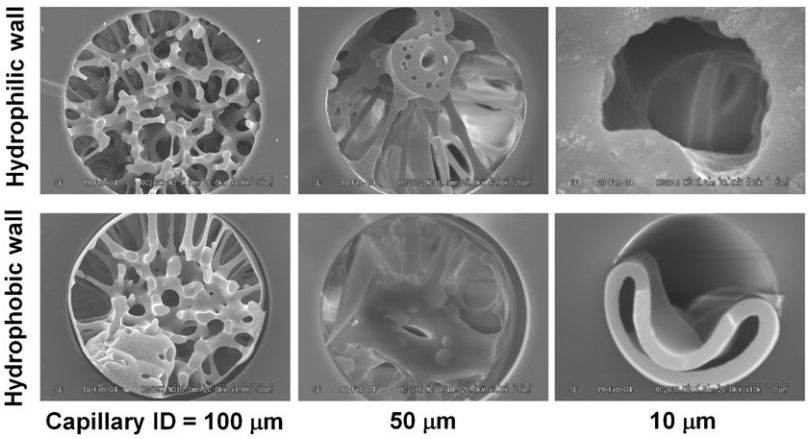

Fig. 11 Macroporous PMSQ gels prepared in capillaries with inner diameters of 100, 50 and 10 μm. The starting composition is MTMS : MeOH : water = 1 : 1.1 : 2.0. Compared to the capillaries with the hydrophilic wall, those with the octadecylsilylated hydrophobic wall contain more deformed structure due to the more accelerated wetting by hydrophobic interaction. Moreover, since no chemical bonds are expected between PMSQ gels and octadecylsilylated walls, thick skin layer can be clearly seen at the interfaces. The wet film in the hydrophobic 10 μm capillary is accidentally collapsed because of the gravity or the capillary force during drying.

of the sol is fixed. In the capillary with a octadecylsilylated hydrophobic wall (lower line in Fig. 11), wetting is accelerated and highly deformed structure is already seen in the capillary with 100 μm diameter. The distinct difference is the presence of a skin layer, which is not strongly bound to the capillary walls because no chemical bonds between PMSQ and octadecylsilylated walls are expected. In both cases, when the length scale of the macroporous structure exceeds the capillary diameter, all of the gel-rich phase is adsorbed onto the capillary wall, showing the wetting transition (see 10 μm capillaries). Some other important factors including the duration between phase separation and gelation, and initial wavelength of spinodal decomposition actually affect the wetting behaviors.[110] Jinnai *et al.* also clearly observed the similar deformation in-between parallel plates in a phase-separating polymer blend system consisting of deuterated polybutadiene (dPB) and PB by a 3-D observation using laser scanning confocal microscopy (LSCM).[113]

We applied the wetting phenomena to the thick-coatings on monolithic columns for the use in HPLC.[107] Although the aforementioned MTMS-derived monolithic columns are excellent in separation properties, they will be further improved if the walls of the macropores, which contain no mesopores, are made porous to improve the loading capacity. On the walls of the monolithic MTMS-derived capillary columns, we prepared a porous silica coating layer by the wetting transition. Since the silica layer was partly peeled-off and collapsed during drying, we evaluated the separation efficiency without undergoing a drying process. The coated monoliths showed a significantly extended retention time in both normal and reversed-phase modes, and it should be attributed to the remaining micropores in the silica layer. The micropores, which usually collapse during drying, strongly adsorb the analyte molecules and retard elution. Recently, Detobel *et al.* succeeded to use the wetting phenomenon to coat the micro-pillar columns,[114,115] which are micro-fabricated on a silicon chip by the photolithography used in the semiconductor industries, with 0.5 μm-thick porous silica.[116] Highly improved separation efficiency would be achieved when the micropores and mesopores in the silica layer can be adequately controlled by methods such as the supramolecular templating and hydrothermal treatment. Furthermore, this technique utilizing anisotropic phase separation is advantageous for coatings of microsurfaces in small geometry, where other techniques such as spin- and dip-coating methods are hard to be performed to form coatings.

By combining wetting phenomena and the gravity effect, it is possible to design a pillar structure inside a capillary with rectangular cross sections.[117] Fig. 12 demonstrates the pillar formation in MTMS–*N*,*N*-dimethylacetamide (DMAc)–NAaq system containing DMAc, which acts as the co-solvent of MTMS-derived condensates and water, that is, increasing amount of DMAc suppresses the phase separation tendency. In a 50 μm gap between parallel plates of the capillary, it can be confirmed that the pillar structure forms as a result of wetting and being stretched by the gravity. This tendency becomes stronger in decreasing the gap of capillary and/or increasing the size of phase-separated structure. Since the decreasing amount of DMAc leads to the higher phase separation tendency, the lateral continuity of the gel phase becomes fewer in decreasing DMAc/MTMS molar ratio as can be seen in the SEM images. Porosity of the pillar structure becomes as high as 0.80 at the middle of the capillary thickness determined by LSCM, and it becomes higher with decreasing DMAc/MTMS ratio. The structural feature and high porosity of the pillar structure allow faster liquid transport as demonstrated in the lower part of Fig. 12. In the case where the PMSQ gel forms a bicontinuous-type structure (at molar ratios DMAc/MTMS = 0.3 and 0.4), pressure drop of the rectangular capillary monolith is as large as a regular capillary monolith with pore diameter of 8 μm. Pressure drop of the commercialized regular capillary monolith MonoCap with pore diameter of 2 μm is even larger due to the small pore size. The rectangular capillary monolith with the pillar structure obtained at DMAc/MTMS = 0.2 shows the considerably small pressure drop, which indicates the possibility of increased linear velocity while maintaining the pressure drop small. The small pressure drop can be attributed to the pillar structure which does not possess

 This journal is © The Royal Society of Chemistry 2011

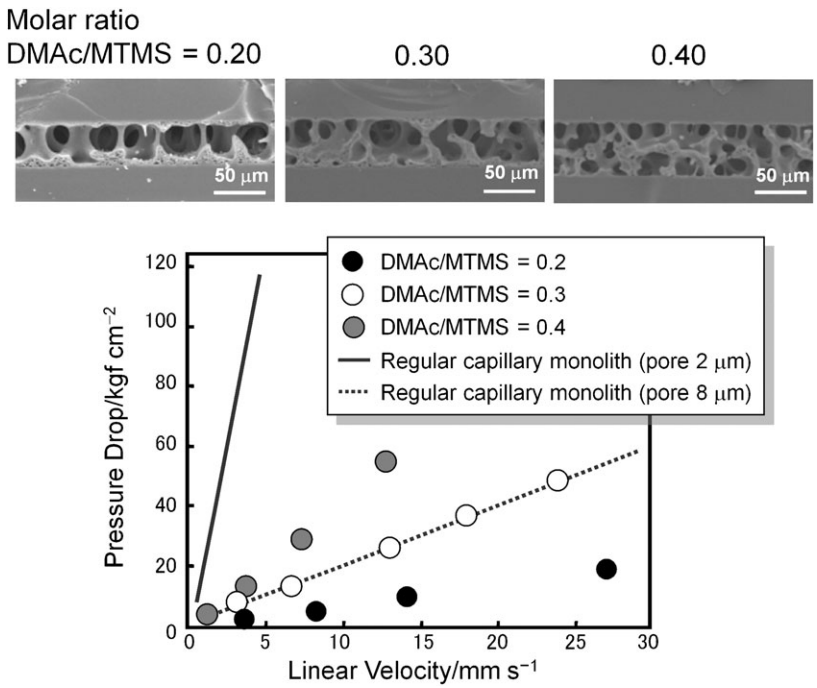

Fig. 12 Pillar structures formed inside capillary with rectangular cross-sections. The molar ratio of the solvent DMAc with respect to MTMS is shown inset and the water-to-MTMS ratio is fixed in 2.5. Relationships between linear velocity and pressure drop measured using a HPLC system are presented in the lower part.

the connections perpendicular to the pillars, and large through-pore size (distance in-between pillars). However, a further improvement of the gel structure such as adjusting through-pore size and increasing specific surface area is required in order to utilize the pillared capillary monolith as an effective separation medium.

4. From aerogels to macro-/mesoporous hybrids

Aerogels[118–124] are a particular class of low-density porous solids characterized by their high porosity ($\sim$90%). Amongst a variety of available chemical compositions as shown later, well-tailored silica aerogels are particularly important for unique properties such as high visible-light transparency (typically $\sim$90%), low density (down to 0.003 g cm^{-3}, only 2–3 times of air),[125] low refractive index, low dielectric constant, *etc*. The low thermal conductivity is derived from the nanometre-sized pores (typically 10–50 nm) with intricate geometry in which heat cannot be transferred by convection and the momentum exchange of gas molecules because the mean free path of air is longer than 60 nm at ambient temperature and pressure. Heat transfer by the solid phase is also suppressed owing to the low fraction of solid phase. As a result, silica aerogels show extremely low thermal conductivity ($<$10 mW m^{-1} K^{-1}), which is the lowest among all solids on earth.[126] This excellent thermal insulation property is expected to help more efficient use of fuel energies and saving natural resources.

Aerogels are prepared with surprisingly wide chemical compositions ranging from inorganic oxides such as silica, alumina, titania, iron oxide (and many others) and their composites,[120–122,127] non-oxides such as chalcogenides,[128] and to organic cross-linked polymers represented by resorcinol–formaldehyde (RF) and melamine–formaldehyde (MF) gels.[123,129,130] The organic polymer aerogels can be converted to carbonaceous aerogels (generally termed as carbon aerogels) through heat treatment in an inert atmosphere. The carbon aerogels are highly promising for applications to catalyst supports[131] and electrodes for electric double-layer capacitors (EDLCs)[132] owing to their huge specific surface areas ($>$2000 m^2 g^{-1})[133] originating from the developed micropores.

Despite of all these unique and excellent properties, silica aerogels are not widely used because of the severe friability arising from the tenuous porous networks in which nanometre-sized particles are weakly connected to each other by touching in a small area, *i.e*. point-contact particles as depicted in Fig. 13. The rigid and brittle silica networks consisting of up to four sp^3 rigid Si–O bonds are another important reason. To maintain the delicate porous structures intact during the drying process of as-prepared wet gels, supercritical drying (SCD), which generates no liquid–gas interfaces and hence no capillary force in the drying material, should be employed using a supercritical fluid. However, the SCD process requires a high-pressure autoclave to reach above the critical point of the fluid. Even for carbon dioxide which has the relatively mild critical condition and hence is often used, the critical pressure is as high as 7.37 MPa ($>$70 atm) with the critical temperature 31.0 °C.

Therefore, in the history of aerogels started from the imaginative invention by Kistler,[134,135] much effort has been paid to improve the low mechanical properties and to avoid dangerous and costly SCD. Most of the effort can be classified into three groups. First, as-prepared wet gels are extensively aged in a mother solution, a monomer solution, or water.[136–138]

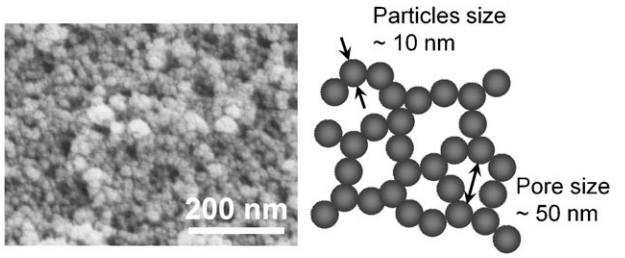

Fig. 13 Typical pore morphology in the nanometre scale in a commercially-available silica aerogel. A schematic 2-D representation is also shown. Each silica nanoparticle, which is typically ~10 nm, connects to form tenuous porous architectures.

It is naturally expected that silica backbones are to some extent reinforced through the neck growth by Ostwald ripening, additional condensation of monomers onto the existing networks, and/or by rearrangement of the as-formed networks. The second group includes hybridization with organic polymers. Novak *et al.*[139] used linear polymers such as poly(2-vinylpyridine) (P2VP), poly(methyl methacrylate-*co*-(3-trimethoxysilyl)propyl methacrylate), and silanol-terminated poly(dimethylsiloxane) in the starting solutions. They also *in situ* polymerized *N*,*N*-dimethylacrylamide in the solution undergoing hydrolysis and polycondensation of silica precursors. Both methods were successful to improve the compressive mechanical properties, and cross-linking of P2VP using copper dichloride is found to be particularly effective. Mackenzie *et al.* employed poly(dimethylsiloxane) with both ends terminated with silanol groups to enhance the flexibility of TEOS-derived aerogels and termed as AEROMOSILs after the name of ORMOSILs (organically modified silicates).[140,141] Leventis *et al.* cross-linked organic polymers using surface reactive groups of aerogels to enhance the mechanical properties and hydrophobicity to be suitable for robust applications (Fig. 14). Native silica aerogels or amino-functionalized silica aerogels using aminopropyltriethoxysilane (APTES) are cross-linked with di-isocyanates,[142] epoxies,[143] and styrenes.[144] Although all these efforts work well to improve the brittleness, hybridization with polymers in general more or less sacrifices optical transparency and porosity.

The third group relies on inclusion of trifunctional silanes. Schubert *et al.* studied monolithic aerogels utilizing TMOS and organotrialkoxysilanes including MTMS, 3-mercaptopropyltrimethoxysilane (MPTMS), 3-glycidoxypropyltrimethoxysilane (GLYMO), 3-methacryloxypropyltrimethoxysilane (MAPTMS), *etc.*[145–147] They observed higher shrinkage and longer gelation time with increasing trialkoxysilanes relative to TMOS due to the less effective and incomplete hydrolysis. In the case of MTMS reacted in basic media, gels were not obtained with higher MTMS ratio (MTMS/TMOS > 0.4). Moreover, in all cases, aerogels became turbid with increasing fractions of trifunctional monomers due to macroscopic phase separation, as is in the case of hybridization with organic polymers as mentioned above. Although only up to 10% of trifunctional silanes (except for MTMS) are effectively included in the silica networks,[146] the surface functional groups can be used for sensors and catalysts. In the case of basic substituent groups such as 3-aminopropyl groups, gelation time was short and the

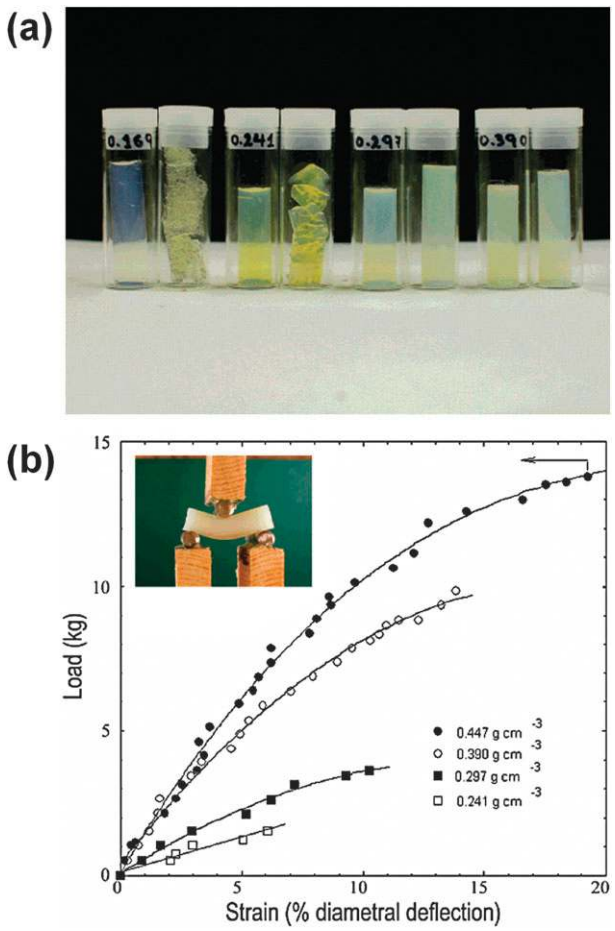

Fig. 14 (a) A picture of four pairs of aerogels. Native silica aerogel (left) and aerogels cross-linked with increasing amount of diisocyanates (from the second left to right). The right side of each pair is the one submerged in liquid nitrogen. (b) Load–strain curves for the four aerogels shown in part (a), demonstrating high mechanical strength against the bending stress. From ref. 142.

trifunctional monomers were completely included in the silica networks, both presumably owing to the hydrogen bonding between amine and silanol groups.[147]

Rao *et al.* also used the mixture of tri- and tetraalkoxysilanes to improve mechanical properties and to gain hydrophobicity. They also found decreases in transparency and specific surface area with increasing MTMS/TMOS ratio and an increase in pore sizes.[148–151] The results are reasonable because increasing MTMS induces macroscopic phase separation because of the increased hydrophobicity of the networks. Contact angle of water droplet reached 175°, showing superhydrophobicity.[150] Since silica aerogels are believed to be sensitive even to the humidity in the air, the surface modification using such as hexamethyldisilazane (HMDS) is required to increase the long-lasting stability.[152] Hydrophobic aerogels derived from organotrialkoxysilanes are therefore advantageous especially for commercial productions because there is no need for such a time- and cost-consuming process. In the case of employing MTMS as the single precursor, flexibility against bending is also noteworthy as shown in Fig. 15,[151] though these aerogels are also opaque due to macroscopic phase separation. When pore

This journal is © The Royal Society of Chemistry 2011

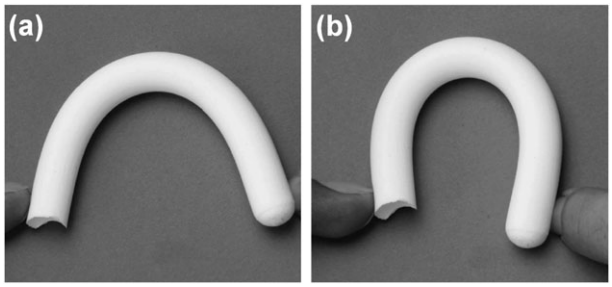

Fig. 15 Flexible PMSQ aerogels obtained from MTMS. Molar ratios of the starting compositions are water/MTMS = 8 and methanol/MTMS = (a) 28 and (b) 35. From ref. 151.

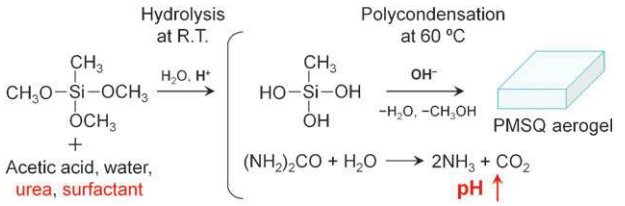

Fig. 16 A modified two-step acid/base reaction for the synthesis of transparent PMSQ aerogels. The single precursor MTMS undergoes hydrolysis in a weakly acidic condition and subsequently pH is raised as a result of hydrolysis of urea for polycondensation in the following step. In addition, adequate surfactant should be added to effectively suppress macroscopic phase separation.

size is increased to, for example, micrometres, high bending flexibility should appear because the volume density of the connecting points in-between the particles decreases and the probability of cracking or collapsing becomes lower. Other groups have found the similar tendency and results in co-gelation systems composed of organotri- and tetraalkoxysilanes.[153–156]

In order to improve optical transparency as well as mechanical properties, we have utilized MTMS as the single precursor for the preparation of PMSQ aerogels.[157–159] We have already pointed out that even a mixture of MTMS and TMOS suffers from opacification because of enhanced macroscopic phase separation. To obtain transparent monolithic aerogels from MTMS, phase separation must be thoroughly inhibited. We hence introduced two important ideas; the modified acid/base two-step reaction and the use of surfactant. In the modified acid/base two-step reaction, almost full and homogeneous hydrolysis is expected in the acid-catalyzed mechanism and the subsequent base-catalyzed reaction, which relies on hydrolysis of urea, allows 3-D network formation in an enhanced manner. In a one-step acid process, the cyclization dominates in the less-branched and slow condensation mechanism, and in the case of one-step base process, precipitation after the slow hydrolysis in basic conditions becomes promoted in a dilute monomer condition which is required for a highly porous aerogels synthesis. Fig. 16 illustrates the modified acid/base two-step reaction conducted as a simple one-pot procedure utilizing urea as a base-releasing agent. The second polycondensation step relies on the generation of ammonia as a result of hydrolysis of aqueous urea at 60 °C. Addition of another base solution in the second step, which is the common way to change the solution pH, gives rise to local pH and allows more rapid growth of condensates than other parts of the solution, which may cause heterogeneity. The employment of urea, which resembles ''precipitation from homogeneous solution'', is crucial for highly isotropic and homogeneous gel formation with preventing formations of cage species. Also employed is a surfactant which effectively suppresses macroscopic phase separation and allows transparent gels to form. In this system, all the components including acetic acid for hydrolysis of MTMS, surfactant, and urea are mixed together as the starting solution. No co-solvent such as alcohols was added, and instead, an excess amount of water is included ($r \approx 15$) both for dilution and hydrolysis of MTMS. After the hydrolysis of MTMS at room temperature, the identical closed reaction vessel is heated at 60 °C to allow the decomposition of urea.

Appearance and some physical properties of the three examples of resultant aerogels are exhibited in Fig. 17 and Table 3. To the best of our knowledge, this is the first example of transparent PMSQ aerogels. Two kinds of surfactants, cationic *n*-hexadecyltrimethylammonium salts (bromide denoted as CTAB and chloride as CTAC), and nonionic triblock copolymer poly(ethylene oxide)-*block*-poly(propylene oxide)-*block*-poly(ethylene oxide) ($EO_{106}PO_{70}EO_{106}$, EO and PO denote ethylene oxide and propylene oxide units, respectively), called as the product name Pluronic F127, are found to be effective in suppressing phase separation. While it is obvious that the compatibility between hydrophobic MTMS-derived networks and the aqueous phase is improved by the surfactant, the detailed mechanism in the molecular level is yet to be clear. Table 3 also shows the higher specific micropore volume W_0 (and therefore higher micropore surface area a_m) for F127-1, suggesting hydrogen bonding between the condensates and EO units in F127 molecules which leaves micropores on removing the penetrated F127 molecules from the network.[160,161] The nano-scaled porous structures are also shown in Fig. 17. The more continuous skeletons with a longer length scale are observed in the PMSQ aerogel prepared with F127, and less continuous skeletons (look more like connected particles as found in the conventional silica aerogels shown in Fig. 13) with a shorter length scale are in the aerogel prepared with CTAB. The difference in transparency between F127-1 and CTAB/CTAC-1 (properties of aerogels are similar between CTAB and CTAC-containing systems) comes mainly from the difference in the length scale and homogeneity of the porous structures.

The important feature of these PMSQ aerogels is the elastic property and high compressive mechanical strength as shown in Fig. 18. The low cross-linking density derived from the trifunctional precursor allows a high deformability, and the methyl groups promote spring-back by repelling each other after the stress is removed. In addition, the low remaining silanol density, which was confirmed by infrared absorption spectra, prevents permanent irreversible shrinkage. The irreversible shrinkage due to the formation of new siloxane bonds upon compression in silica gels is universally observed.[162] This unfavorable phenomenon was successfully avoided by the hybrid networks. The stress–strain curve obtained from a uniaxial compression test demonstrates that

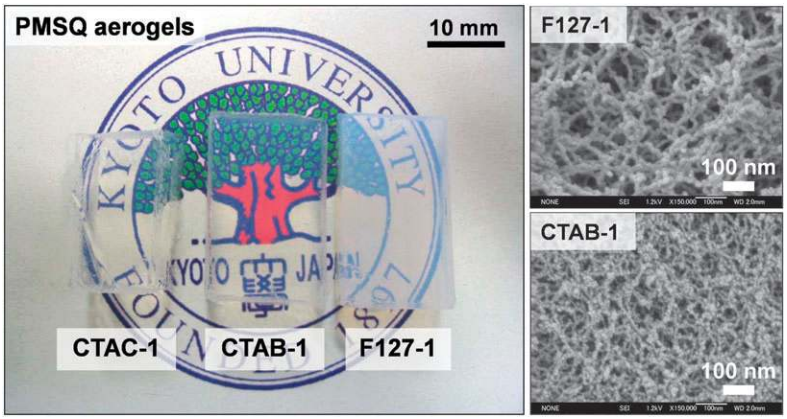

Fig. 17 Appearance of three PMSQ aerogels prepared under the co-presence of CTAC, CTAB, and Pluronic F127 surfactants. These aerogels are obtained by supercritical drying. For starting compositions, see Table 3. Porous structures for F127-1 and CTAB-1 are also exhibited.

Table 3 Physical properties of the obtained PMSQ aerogels[a]

Code	ρ_b[b]/g cm^{-3}	ε_p[c] (%)	T[d] (%)	a_{BET}[e]/m^2 g^{-1}	a_m[f]/m^2 g^{-1}	W_0[g]/cm^3 g^{-1}	V_p[h]/cm^3 g^{-1}
CTAB-1	0.13	91	89	601	148	0.080	6.9
CTAC-1	0.14	90	87	618	141	0.074	6.4
F127-1	0.17	88	39	528	220	0.11	5.0

[a] Starting compositions are; MTMS 10 mL, aqueous acetic acid 20 mL, urea 6.0 g and surfactant. The amounts of surfactant are; CTAB 0.80 g (CTAB-1), CTAC 0.80 g (CTAC-1) and F127 2.0 g (F127-1). Note that the concentration of acetic acid is 1 mM for CTAB-1 and CTAC-1, and 5 mM for F127-1. [b] Bulk density. [c] Porosity. [d] Light transmittance at 550 nm through a 10 mm thick-equivalent sample. [e] BET total surface area determined by nitrogen adsorption/desorption at 77 K. [f] Micropore surface area determined by α_s-plot. [g] Micropore volume by α_s-plot. [h] Total pore volume determined from the true density (1.41 g cm^{-3}) and bulk density.

the PMSQ aerogel can be compressed up to 80% with a stress of >9 MPa and recovers to its original size after removing the load; resilience for optimized gels reaches almost 100%. With the aid of the spring-back phenomenon, the wet PMSQ gels can be dried from solvents with low surface energy simply by evaporation in an ambient condition with undergoing

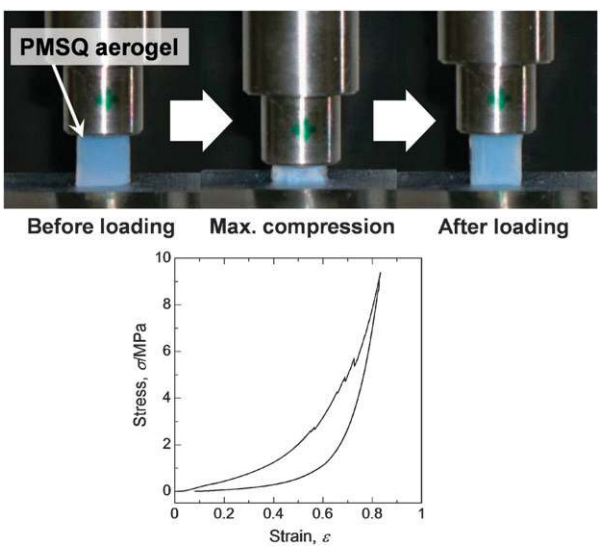

Fig. 18 Overview of the temporal shrinkage and spring-back behavior during a uniaxial compression test of a PMSQ aerogel prepared with CTAB. A stress–strain curve of the identical aerogel is also shown. A nearly perfect elastic behavior (98% final resilience in this case) can be confirmed, though some chipping on the surface occurs.

temporal shrinkage and reexpansion, and aerogel-like xerogels are successfully obtained.[157] Density, light transmittance, porous and mechanical properties are almost equivalent between supercritically-dried aerogels and evaporatively-dried xerogels. Further, huge PMSQ aerogel tiles can be obtained without cracking and shrinkage, which will be reported in the near future.

These PMSQ aerogels are flexible against the compressive stress as described; however, they are friable against the tensile stress. Further improvement by post-treatment and/or co-gelation with other network-forming precursors would be required to tailor truly flexible and bendable aerogels. It should be noted that aerogels consisting of bridged polysilsesquioxanes derived from α,ω-bis(triethoxysilyl)alkanes[163] do not imply this kind of elastic mechanical properties such as large temporal shrinkage and reexpansion on applying a large stress. Other systems consisting of arylene-bridged polysilsesquioxane also show large shrinkage upon evaporative drying.[164] In the silica aerogel films with surface functionalization using trimethylchlorosilane, spring-back behavior is reported and 98.5% porosity is achieved without supercritical drying.[165] However, to allow 3-D spring-back to occur in monoliths without causing physical damage, the presence of the dangling hydrophobic groups, low remaining silanol density, and the low cross-linking density are the requisite factors.

Recently, a bridge connecting these aerogels and phase-separated macroporous gels has been also constructed.[166] In the system containing F127, reduction in the amount of F127 causes macroscopic phase separation and well-defined

 This journal is © The Royal Society of Chemistry 2011

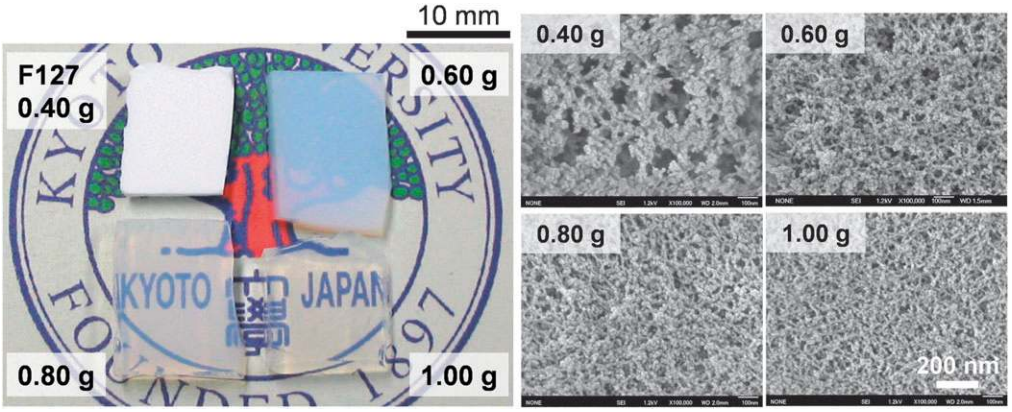

Fig. 19 Appearance of the aerogels obtained with decreasing amounts of Pluronic F127 (amounts shown inset). Other compositions; MTMS 5 mL, 5 mM aqueous acetic acid 6 mL, and urea 0.50 g. It is confirmed that the aerogels become turbid with decreasing amount of F127 because of the insufficient suppression of macroscopic phase separation. The FE-SEM images show the transition of porosity from uniform mesopores (1.00 g) to pores influenced by macroscopic phase separation (0.40 g).

macropores are regulated. Fig. 19 demonstrates the reduction in transparency with decreasing amount of F127. Pore size is confirmed to be increased with decreasing F127 from 30 nm (F127 1.00 g) to over 100 nm (0.40 g) determined both from microscopy (Fig. 19) and nitrogen adsorption–desorption measurements, due to the enhanced macroscopic phase separation. With further decreasing F127, macroscopic phase separation becomes dominant, and micrometre-sized macropores with well-defined bicontinuous structure are resulted as shown in Fig. 20. In the skeletons of the macropores, mesopores around 10 nm in size and 0.2–0.4 $cm^3\ g^{-1}$ in volume with BET specific surface area $>400\ m^2\ g^{-1}$ are still left as a result of microscopic phase separation. In the strong-acid-catalyzed systems mentioned in Section 3, the nitrogen adsorption–desorption isotherms are all type I and we did not find any mesopores but only micropores in the macropore skeletons. In an acid-catalyzed system, since less-branched linear-like polymers form as a result of the slower condensation preferentially taking place in the terminal silanols.[167] In such a polymeric network, together with the relatively high volume fraction of monomers (for MTMS–MeOH–NAaq system, volume fraction of MTMS/(entire sol) is typically $\sim$0.7), mesopores are hard to be formed in the relatively dense networks swollen with only a small amount of solvent. In a base-catalyzed condensation, on the other hand, highly branched colloid-like polymers form as a result of the faster condensation in more-branched silanol species, resulting in inter-particles mesopores formed in the colloidal networks. In the present case, mesopores are not directed by the surfactant micelles, but are formed as a result of microphase separation of colloidal PMSQ from the solvent. Since the amount of solvent, which mainly determines the mesopore size and volume, in the gelling phase is dependent on the progress of macroscopic phase separation, simultaneous fine control of size and volume of both mesopores and macropores may not be easy. However, we believe that this system gives a chance to establish a wide control of hierarchical porosity in the organotrialkoxysilanes-derived sol–gel systems, which has not been done so far.

Hüsing *et al*. also studied the formation of hierarchically pore structures through a unique process using glycol-modified organosilanes in the presence of lyotropic liquid crystalline (LC) phases of aqueous surfactant solution.[168,169] Starting from organotrialkoxysilanes such as MTMS and phenyltrimethoxysilane (PTMS), the alkoxy groups are replaced with various diols and polyols such as ethylene glycol and glycerol through the transalkoxylation reaction. The glycol-modified organosilanes are reacted in the LC media with or without glycol-modified silanes prepared from tetraalkoxysilanes. The modified silanes are reported to be advantageous in obtaining hierarchically porous monoliths because they offer rapid reaction rate even without catalysts (*e.g*. in neutral conditions) and the hydrolysis products as diols or polyols show a good compatibility with the existing LC phases. With increasing ratio of modified methyl- or phenylsilanes, they found decreasing long-range periodicity and increasing gelation time. In monoliths prepared only from the glycol-modified methylsilane in pH = 2, no mesoporosity is reported.

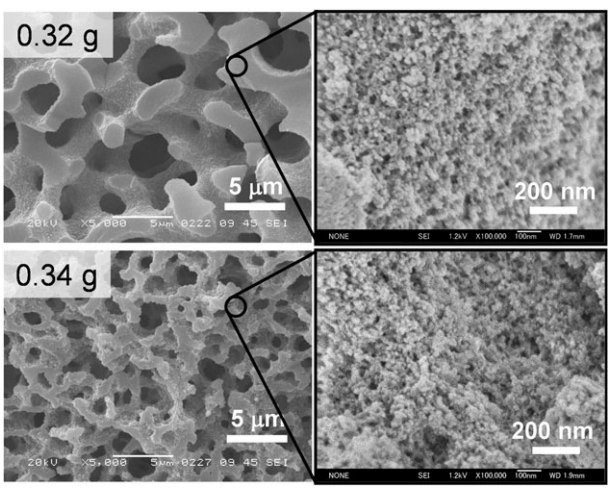

Fig. 20 With further decreasing amount of Pluronic F127, well-defined macroporous structure is observed. In these well-defined macroporous PMSQ gels, mesopores are found by nitrogen adsorption–desorption with *ca*. 400 $m^2\ g^{-1}$ of BET specific surface area.

To these complex systems accompanied by concurrent several phenomena such as colloidal aggregation, phase separation and gelation, much attention will be paid because of the potential importance in controlling the hierarchical pore structures in organotrialkoxysilanes-derived gels through rich science.

5. Summary and future perspectives

A brief overview of recent trifunctional silanes-derived porous materials is described featuring those explored by the authors as well as other groups. In both academic and industrial fields, though the trifunctional monomers in sol–gel chemistry may often be regarded as non-gelling precursors, a source of silicone resins, or as a surface modifier, the authors believe these precursors leave considerably attracting features including surface and mechanical properties. In addition to the well-known fact that trifunctional silanes with hydrophilic functional substituents such as amino and epoxy groups are relatively easy to be incorporated in the siloxane-based networks and provide the surface functionality, those with small hydrophobic substituents realize unique mechanical properties as demonstrated in the study of PMSQ aerogels. Also, in terms of applications in engineering and technology, it is revealed that the PMSQ materials are highly important for their low-k properties and for amphiphilic surface properties that allow separation of both hydrophobic and hydrophilic molecules in HPLC applications.

Alkoxysilanes with short aliphatic or aromatic groups are becoming more and more popular for tailoring monolithic porous materials such as aerogels or for preparing low-k films, but their pore formability is largely unexplored. Macropores and mesopores without crystalline symmetries can be formed in adequately controlled conditions as discussed in this review. However, polysilsesquioxanes with ordered mesopores from these precursors have not been unveiled. Although we have to keep in mind that there is an inherent difficulty resulting from the fact that there are only few available silanol sites and unable to interact with structure-directing agents, we expect a splendid progress will be achieved by excellent research contributions from all over the world.

Acknowledgements

The authors wish to acknowledge Grant-in-Aid for Scientific Research from Japan Society for the Promotion of Science (JSPS) and Ministry of Education, Culture, Sports, Science and Technology (MEXT), Japan. Also acknowledged is the financial supports from Global COE program ''International Center for Integrated Research and Advanced Education in Materials Science'' (No. B-09) of the MEXT, administrated by JSPS. Part of this work was entrusted by the New Energy and Industrial Technology Development Organization (NEDO) as 'the Project of Development of Multiceramic Film for New Thermal Insulators'.

Notes and references

1 C. J. Brinker and G. W. Scherer, *Sol–Gel Science: The Physics and Chemistry of Sol-Gel Processing*, Academic Press, San Diego, CA, 1990.
2 B. M. Novak, *Adv. Mater.*, 1993, **5**, 422–433.
3 U. Schubert, N. Hüsing and A. Lorenz, *Chem. Mater.*, 1995, **7**, 2010–2027.
4 J. Wen and G. L. Wilkes, *Chem. Mater.*, 1996, **8**, 1667–1681.
5 J. Pyun and K. Matyjaszewski, *Chem. Mater.*, 2001, **13**, 3436–3448.
6 D. Avnir, T. Coradin, O. Lev and J. Livage, *J. Mater. Chem.*, 2006, **16**, 1013–1030.
7 A. Shimojima and K. Kuroda, *Chem. Rec.*, 2006, **6**, 53–63.
8 G. J. A. A. Soler-Illia and P. Innocenzi, *Chem.–Eur. J.*, 2006, **12**, 4478–4494.
9 J. D. Mackenzie and E. P. Bescher, *Acc. Chem. Res.*, 2007, **40**, 810–818.
10 C. Sanchez, L. Rozes, F. Ribot, C. Laberty-Robert, D. Grosso, C. Sassoye, C. Boissiere and L. Nicole, *C. R. Chim.*, 2010, **13**, 3–39.
11 D. A. Loy and K. J. Shea, *Chem. Rev.*, 1995, **95**, 1431–1442.
12 R. J. P. Corriu and D. Leclercq, *Angew. Chem., Int. Ed. Engl.*, 1996, **35**, 1420–1436.
13 D. A. Loy, B. M. Baugher, C. R. Baugher, D. A. Schneider and K. Rahimian, *Chem. Mater.*, 2000, **12**, 3624–3632.
14 K. J. Shea and D. A. Loy, *Chem. Mater.*, 2001, **13**, 3306–3319.
15 R. H. Baney, M. Itoh, A. Sakakibara and T. Suzuki, *Chem. Rev.*, 1995, **95**, 1409–1430.
16 J. F. Brown, Jr., L. H. Vogt, Jr., A. Katchman, J. W. Eustance, K. M. Kiser and K. W. Krantz, *J. Am. Chem. Soc.*, 1960, **82**, 6194–6195.
17 M. Unno, A. Suto and H. Matsumoto, *J. Am. Chem. Soc.*, 2002, **124**, 1574–1575.
18 M. Unno, R. Tanaka, S. Tanaka, T. Takeuchi, S. Kyushin and H. Matsumoto, *Organometallics*, 2005, **24**, 765–768.
19 K. Suyama, T. Gunji, K. Arimitsu and Y. Abe, *Organometallics*, 2006, **25**, 5587–5593.
20 J. Livage and M. Henry, in *Ultrastructure Processing of Advanced Ceramics*, ed. J. D. Mackenzie and D. R. Ulrich, John Wiley & Sons, New York, NY, 1988, pp. 183–195.
21 E. J. Little, Jr. and M. M. Jones, *J. Chem. Educ.*, 1960, **37**, 231–233.
22 N. Inamoto and S. Masuda, *Chem. Lett.*, 1982, 1003–1006.
23 D. A. Loy, J. P. Carpenter, S. A. Myers, R. A. Assink, J. H. Small, J. Greaves and K. J. Shea, *J. Am. Chem. Soc.*, 1996, **118**, 8501–8502.
24 D. A. Loy, J. P. Carpenter, T. M. Alam, R. Shaltout, P. K. Dorhout, J. Greaves, J. H. Small and K. J. Shea, *J. Am. Chem. Soc.*, 1999, **121**, 5413–5425.
25 J. J. Schwab and J. D. Lichtenhan, *Appl. Organomet. Chem.*, 1998, **12**, 707–713.
26 G. Li, L. Wang, H. Ni and C. U. Pittman Jr., *J. Inorg. Organomet. Polym.*, 2001, **11**, 123–154.
27 D. B. Cordes, P. D. Lickiss and F. Rataboul, *Chem. Rev.*, 2010, **110**, 2081–2173.
28 P. A. Agaskar, *Inorg. Chem.*, 1991, **30**, 2707–2708.
29 K. Pielichowski, J. Njuguna, B. Janowski and J. Pielichowski, *Adv. Polym. Sci.*, 2006, **201**, 225–296.
30 D. Hoebbel, K. Endres, T. Reinert and I. Pitsch, *J. Non-Cryst. Solids*, 1994, **176**, 179–188.
31 C. Zhang, F. Babonneau, C. Bonhomme, R. M. Laine, C. L. Soles, H. A. Hristov and A. F. Yee, *J. Am. Chem. Soc.*, 1998, **120**, 8380–8391.
32 L. Zhang, H. C. L. Abbenhuis, Q. Yang, Y.-M. Wang, P. C. M. M. Magusin, B. Mezari, R. A. van Santen and C. Li, *Angew. Chem., Int. Ed.*, 2007, **46**, 5003–5006.
33 Y. Hagiwara, A. Shimojima and K. Kuroda, *Chem. Mater.*, 2008, **20**, 1147–1153.
34 Y. Hagiwara, A. Shimojima and K. Kuroda, *Bull. Chem. Soc. Jpn.*, 2010, **83**, 424–430.
35 S. Che, A. E. Garcia-Bennett, T. Yokoi, K. Sakamoto, H. Kunieda, O. Terasaki and T. Tatsumi, *Nat. Mater.*, 2003, **2**, 801–805.
36 S. Che, Z. Liu, T. Ohsuna, K. Sakamoto, O. Terasaki and T. Tatsumi, *Nature*, 2004, **429**, 281–284.
37 H. Jin, Z. Liu, T. Ohsuna, O. Terasaki, Y. Inoue, K. Sakamoto, T. Nakanishi, K. Ariga and S. Che, *Adv. Mater.*, 2006, **18**, 593–596.
38 C. Gao, Y. Sakamoto, O. Terasaki, K. Sakamoto and S. Che, *J. Mater. Chem.*, 2007, **17**, 3591–3602.

 This journal is © The Royal Society of Chemistry 2011

39 R. Atluri, N. Hedin and A. E. Garcia-Bennett, *J. Am. Chem. Soc.*, 2009, **131**, 3189–3191.
40 M. H. Lim, C. F. Blanford and A. Stein, *Chem. Mater.*, 1998, **10**, 467–470.
41 K. Wilson, A. F. Lee, D. J. Macquarrie and J. H. Clark, *Appl. Catal., A*, 2002, **228**, 127–133.
42 V. Ganesan and A. Walcarius, *Langmuir*, 2004, **20**, 3632–3640.
43 A. Walcarius and V. Ganesan, *Langmuir*, 2006, **22**, 469–477.
44 H.-Y. Wu, C.-H. Liao, Y.-C. Pan, C.-L. Yeh and H.-M. Kao, *Microporous Mesoporous Mater.*, 2009, **119**, 109–116.
45 L. Beaudet, R. Pitre, L. Robillard and L. Mercier, *Chem. Mater.*, 2009, **21**, 5349–5357.
46 F. O. M. Gaslain, C. Delacôte, A. Walcarius and B. Lebeau, *J. Sol-Gel Sci. Technol.*, 2009, **49**, 112–124.
47 A. Katz and M. E. Davis, *Nature*, 2000, **403**, 286–289.
48 M. C. Burleigh, S. Dai, E. W. Hagaman and J. S. Lin, *Chem. Mater.*, 2001, **13**, 2537–2546.
49 A. S. M. Chong and X. S. Zhao, *J. Phys. Chem. B*, 2003, **107**, 12650–12657.
50 Z. Luan, J. A. Fournier, J. B. Wooten and D. E. Miser, *Microporous Mesoporous Mater.*, 2005, **83**, 150–158.
51 J. Moreno and D. C. Sherrington, *Chem. Mater.*, 2008, **20**, 4468–4474.
52 R. M. Grudzien, S. Pikus and M. Jaroniec, *J. Phys. Chem. C*, 2009, **113**, 4875–4884.
53 Y. Ide, G. Ozaki and M. Ogawa, *Langmuir*, 2009, **25**, 5276–5281.
54 T. Borrego, M. Andrade, M. L. Pinto, A. R. Silva, A. P. Carvalho, J. Rocha, C. Freire and J. Pires, *J. Colloid Interface Sci.*, 2010, **344**, 603–610.
55 C. D. Nunes, A. A. Valente, M. Pillinger, A. C. Fernandes, C. C. Romão, J. Rocha and I. S. Gonçalves, *J. Mater. Chem.*, 2002, **12**, 1735–1742.
56 C. M. Crudden, M. Sateesh and R. Lewis, *J. Am. Chem. Soc.*, 2005, **127**, 10045–10050.
57 X. Wang, K. S. K. Lin, J. C. C. Chan and S. Cheng, *J. Phys. Chem. B*, 2005, **109**, 1763–1769.
58 K. Feng, R.-Y. Zhang, L.-Z. Wu, B. Tu, M.-L. Peng, L.-P. Zhang, D. Zhao and C.-H. Tung, *J. Am. Chem. Soc.*, 2006, **128**, 14685–14690.
59 K. Szymańska, J. Bryjak, J. Mrowiec-Białoń and A. B. Jarzębski, *Microporous Mesoporous Mater.*, 2007, **99**, 167–175.
60 C. M. Crudden, K. McEleney, S. L. MacQuarrie, A. Blanc, M. Sateesh and J. D. Webb, *Pure Appl. Chem.*, 2007, **79**, 247–260.
61 K. K. Sharma, A. Anan, R. P. Buckley, W. Ouellette and T. Asefa, *J. Am. Chem. Soc.*, 2008, **130**, 218–228.
62 L.-H. Hsiao, S.-Y. Chen, S.-J. Huang, S.-B. Liu, P.-H. Chen, J. C.-C. Chan and S. Cheng, *Appl. Catal., A*, 2009, **359**, 96–107.
63 M. Mureseanu, A. Reiss, I. Stefanescu, E. David, V. Parvulescu, G. Renard and V. Hulea, *Chemosphere*, 2008, **73**, 1499–1504.
64 J. Li, X. Miao, Y. Hao, J. Zhao, X. Sun and L. Wang, *J. Colloid Interface Sci.*, 2008, **318**, 309–314.
65 S. Srisuda and B. Virote, *J. Environ. Sci.*, 2008, **20**, 379–384.
66 Z. Chen and T. Hobo, *Anal. Chem.*, 2001, **73**, 3348–3357.
67 B. Preinerstorfer, D. Lubda, W. Lindner and M. Lämmerhofer, *J. Chromatogr., A*, 2006, **1106**, 94–105.
68 M. D. Slater, J. M. J. Fréchet and F. Svec, *J. Sep. Sci.*, 2009, **32**, 21–28.
69 Y. Tian, W. Lu, Y. Che, L. B. Shen, L. M. Jiang and Z. Q. Shen, *J. Appl. Polym. Sci.*, 2010, **115**, 999–1007.
70 W. Xu, H. Guo and D. L. Akins, *J. Phys. Chem. B*, 2001, **105**, 1543–1546.
71 W. Xu, Y. Liao and D. L. Akins, *J. Phys. Chem. B*, 2002, **106**, 11127–11131.
72 L.-N. Sun, H.-J. Zhang, J.-B. Yu, S.-Y. Yu, C.-Y. Peng, S. Dang, X.-M. Guo and J. Feng, *Langmuir*, 2008, **24**, 5500–5507.
73 F. Hoffmann, M. Cornelius, J. Morell and M. Fröba, *Angew. Chem., Int. Ed.*, 2006, **45**, 3216–3251.
74 S. S. Park and C.-S. Ha, *Chem. Rec.*, 2006, **6**, 32–42.
75 Q. Yang, J. Liu, L. Zhang and C. Li, *J. Mater. Chem.*, 2009, **19**, 1945–1955.
76 P. Kumar and V. V. Guliants, *Microporous Mesoporous Mater.*, 2010, **132**, 1–14.
77 G. Schottner, *Chem. Mater.*, 2001, **13**, 3422–3435.
78 L. Nicole, L. Rozes and C. Sanchez, *Adv. Mater.*, 2010, **22**, 3208–3214.
79 A. Shimojima and K. Kuroda, *J. Sol-Gel Sci. Technol.*, 2008, **46**, 307–311.
80 A. Shimojima, *J. Ceram. Soc. Jpn.*, 2008, **116**, 278–283.
81 K. Kanamori, H. Yonezawa, K. Nakanishi, K. Hirao and H. Jinnai, *J. Sep. Sci.*, 2004, **27**, 874–886.
82 K. Nakanishi and K. Kanamori, *J. Mater. Chem.*, 2005, **15**, 3776–3786.
83 A. Itagaki, K. Nakanishi and K. Hirao, *J. Sol-Gel Sci. Technol.*, 2003, **26**, 153–156.
84 K. Nakanishi, *J. Porous Mater.*, 1997, **4**, 67–112.
85 K. Nakanishi and N. Tanaka, *Acc. Chem. Res.*, 2007, **40**, 863–873.
86 H. Kaji, K. Nakanishi and N. Soga, *J. Non-Cryst. Solids*, 1995, **181**, 16–26.
87 H. Kaji, K. Nakanishi and N. Soga, *J. Non-Cryst. Solids*, 1995, **185**, 18–30.
88 p. 141 in ref. 1 and references therein.
89 H. Dong, M. A. Brook and J. D. Brennan, *Chem. Mater.*, 2005, **17**, 2807–2816.
90 H. Dong and J. D. Brennan, *Chem. Mater.*, 2006, **18**, 541–546.
91 H. Dong and J. D. Brennan, *Chem. Mater.*, 2006, **18**, 4176–4182.
92 S. Kumon, K. Nakanishi and K. Hirao, *J. Sol-Gel Sci. Technol.*, 2000, **19**, 553–557.
93 K. Nakanishi, *J. Sol-Gel Sci. Technol.*, 2000, **19**, 65–70.
94 K. Kanamori, N. Ishizuka, K. Nakanishi, K. Hirao and H. Jinnai, *J. Sol-Gel Sci. Technol.*, 2003, **26**, 157–160.
95 K. Kanamori, K. Nakanishi, K. Hirao and H. Jinnai, *Langmuir*, 2003, **19**, 5581–5585.
96 K. Kanamori, K. Nakanishi, K. Hirao and H. Jinnai, *Colloids Surf., A*, 2004, **241**, 215–224.
97 T. Tanaka, N. Kawakami, T. Hirano, Y. Fukumoto, T. Suzuki, K. Kanamori and K. Nakanishi, *Mater. Res. Soc. Symp. Proc.*, 2006, **888**, V09-17.1.
98 K. Maex, M. R. Baklanov, D. Shamiryan, F. Iacopi, S. H. Brongersma and Z. S. Yanovitskaya, *J. Appl. Phys.*, 2003, **93**, 8793–8841.
99 L. Nicole, C. Boissiére, D. Grosso, A. Quach and C. Sanchez, *J. Mater. Chem.*, 2005, **15**, 3598–3627.
100 B. D. Hatton, K. Landskron, W. J. Hunks, M. R. Bennett, D. Shukaris, D. D. Perovic and G. A. Ozin, *Mater. Today*, 2006, **9**, 22–31.
101 W. Volksen, R. D. Miller and G. Dubois, *Chem. Rev.*, 2010, **110**, 56–110.
102 A. R. Balkenende, F. K. de Theije and J. C. K. Kriege, *Adv. Mater.*, 2003, **15**, 139–143.
103 F. K. de Theije, A. R. Balkenende, M. A. Verheijen, M. R. Baklanov, K. P. Mogilnikov and Y. Furukawa, *J. Phys. Chem. B*, 2003, **107**, 4280–4289.
104 M. Matheron, A. Bourgeois, A. Brunet-Bruneau, P.-A. Albouy, J. Biteau, T. Gacoin and J.-P. Boilot, *J. Mater. Chem.*, 2005, **15**, 4741–4745.
105 M. Matheron, T. Gacoin and J.-P. Boilot, *Soft Matter*, 2007, **3**, 223–229.
106 G. J. A. A. Soler-Illia, C. Sanchez, B. Lebeau and J. Patarin, *Chem. Rev.*, 2002, **102**, 4093–4138.
107 K. Kanamori, K. Nakanishi and T. Hanada, *J. Sep. Sci.*, 2006, **29**, 2463–2470.
108 K. Kanamori, K. Nakanishi, K. Hirao and H. Jinnai, *Langmuir*, 2003, **19**, 9101–9103.
109 K. Kanamori, K. Nakanishi, K. Hirao and H. Jinnai, *J. Sol-Gel Sci. Technol.*, 2005, **35**, 183–191.
110 K. Kanamori, K. Nakanishi and T. Hanada, *Soft Matter*, 2009, **5**, 3106–3113.
111 H. Tanaka, *J. Phys.: Condens. Matter*, 2001, **13**, 4637–4674.
112 M. Geoghegan and G. Krausch, *Prog. Polym. Sci.*, 2003, **28**, 261–302.
113 H. Jinnai, H. Kitagishi, K. Hamano, Y. Nishikawa and M. Takahashi, *Phys. Rev. E: Stat., Nonlinear, Soft Matter Phys.*, 2003, **67**, 021801.
114 B. He, N. Tait and F. Regnier, *Anal. Chem.*, 1998, **70**, 3790–3797.
115 F. E. Regnier, *J. High Resolut. Chromatogr.*, 2000, **23**, 19–26.
116 F. Detobel, H. Eghbali, S. De Bruyne, H. Terryn, H. Gardeniers and G. Desmet, *J. Chromatogr., A*, 2009, **1216**, 7360–7367.
117 Y. Suzumura, K. Kanamori, K. Nakanishi, K. Hirao and J. Yamamichi, *J. Chromatogr., A*, 2006, **1119**, 88–94.

118 H. D. Gesser and P. C. Goswami, *Chem. Rev.*, 1989, **89**, 765–788.
119 J. Fricke and A. Emmerling, *J. Am. Ceram. Soc.*, 1992, **75**, 2027–2036.
120 N. Hüsing and U. Schubert, *Angew. Chem., Int. Ed.*, 1998, **37**, 22–45.
121 D. R. Rolison and B. Dunn, *J. Mater. Chem.*, 2001, **11**, 963–980.
122 A. C. Pierre and G. M. Pajonk, *Chem. Rev.*, 2002, **102**, 4243–4265.
123 S. A. Al-Muhtaseb and J. A. Ritter, *Adv. Mater.*, 2003, **15**, 101–114.
124 J. W. Long and D. R. Rolison, *Acc. Chem. Res.*, 2007, **40**, 854–862.
125 T. M. Tillotson and L. W. Hrubesh, *J. Non-Cryst. Solids*, 1992, **145**, 44–50.
126 B. E. Yoldas, M. J. Annen and J. Bostaph, *Chem. Mater.*, 2000, **12**, 2475–2484.
127 C. A. Morris, M. L. Anderson, R. M. Stroud, C. I. Merzbacher and D. R. Rolison, *Science*, 1999, **284**, 622–624.
128 J. L. Mohanan, I. U. Arachchige and S. L. Brock, *Science*, 2005, **307**, 397–400.
129 R. W. Pekala, *J. Mater. Sci.*, 1989, **24**, 3221–3227.
130 R. W. Pekala, C. T. Alviso, F. M. Kong and S. S. Hulsey, *J. Non-Cryst. Solids*, 1992, **145**, 90–98.
131 C. Moreno-Castilla and F. J. Maldonado-Hódar, *Carbon*, 2005, **43**, 455–465.
132 E. Frackowiak and F. Béguin, *Carbon*, 2001, **39**, 937–950.
133 Y. Hanzawa, K. Kaneko, R. W. Pekala and M. S. Dresselhaus, *Langmuir*, 1996, **12**, 6167–6169.
134 S. S. Kistler, *Nature*, 1931, **127**, 741.
135 S. S. Kistler, *J. Phys. Chem.*, 1932, **36**, 52–64.
136 S. Hæreid, J. Anderson, M. A. Einarsrud, D. W. Hua and D. M. Smith, *J. Non-Cryst. Solids*, 1995, **185**, 221–226.
137 S. Hæreid, M. Dahle, S. Lima and M.-A. Einarsrud, *J. Non-Cryst. Solids*, 1995, **186**, 96–103.
138 G. Reichenauer, *J. Non-Cryst. Solids*, 2004, **350**, 189–195.
139 B. M. Novak, D. Auerbach and C. Verrier, *Chem. Mater.*, 1994, **6**, 282–286.
140 S. J. Kramer, F. Rubio-Alonso and J. D. Mackenzie, *Mater. Res. Soc. Symp. Proc.*, 1996, **435**, 295–300.
141 J. D. Mackenzie and E. P. Bescher, in: *Handbook of Sol-Gel Science and Technology: Processing Characterization and Applications*, ed. S. Sakka (Volume ed. R. M. Almeida), Kluwer Academic Publishers, Dordrecht, 2004, vol. II, pp. 313–326.
142 N. Leventis, C. Sotiriou-Leventis, G. Zhang and A.-M. M. Rawashdeh, *Nano Lett.*, 2002, **2**, 957–960.
143 M. A. B. Meador, E. F. Fabrizio, F. Ilhan, A. Dass, G. Zhang, P. Vassilaras, J. C. Johnston and N. Leventis, *Chem. Mater.*, 2005, **17**, 1085–1098.
144 U. F. Ilhan, E. F. Fabrizio, L. McCorkle, D. A. Scheiman, A. Dass, A. Palczer, M. A. B. Meador, J. C. Johnston and N. Leventis, *J. Mater. Chem.*, 2006, **16**, 3046–3054.
145 F. Schwertfeger, W. Glaubitt and U. Schubert, *J. Non-Cryst. Solids*, 1992, **145**, 85–89.
146 N. Hüsing, U. Schubert, K. Misof and P. Fratzl, *Chem. Mater.*, 1998, **10**, 3024–3032.
147 N. Hüsing, U. Schubert, R. Mezei, P. Fratzl, B. Riegel, W. Kiefer, D. Kohler and W. Mader, *Chem. Mater.*, 1999, **11**, 451–457.
148 A. V. Rao and D. Haranath, *Microporous Mesoporous Mater.*, 1999, **30**, 267–273.
149 A. V. Rao and G. M. Pajonk, *J. Non-Cryst. Solids*, 2001, **285**, 202–209.
150 A. V. Rao, G. M. Pajonk, S. D. Bhagat and P. Barboux, *J. Non-Cryst. Solids*, 2004, **350**, 216–223.
151 A. V. Rao, S. D. Bhagat, H. Hirashima and G. M. Pajonk, *J. Colloid Interface Sci.*, 2006, **300**, 279–285.
152 H. Yokogawa and M. Yokoyama, *J. Non-Cryst. Solids*, 1995, **186**, 23–29.
153 H. E. Rassy, P. Buisson, B. Bouali, A. Perrard and A. C. Pierre, *Langmuir*, 2003, **19**, 358–363.
154 T. M. Tillotson, K. G. Foster and J. G. Reynolds, *J. Non-Cryst. Solids*, 2004, **350**, 209–215.
155 L. Martín, J. O. Ossó, S. Ricart, A. Roig, O. García and R. Sastre, *J. Mater. Chem.*, 2008, **18**, 207–213.
156 H. Guo, B. N. Nguyen, L. S. McCorkle, B. Shonkwiler and M. A. B. Meador, *J. Mater. Chem.*, 2009, **19**, 9054–9062.
157 K. Kanamori, M. Aizawa, K. Nakanishi and T. Hanada, *Adv. Mater.*, 2007, **19**, 1589–1593.
158 K. Kanamori, M. Aizawa, K. Nakanishi and T. Hanada, *J. Sol-Gel Sci. Technol.*, 2008, **48**, 172–181.
159 K. Kanamori, K. Nakanishi and T. Hanada, *J. Ceram. Soc. Jpn.*, 2009, **117**, 1333–1338.
160 R. Ryoo, C. H. Ko, M. Kruk, V. Antochshuk and M. Jaroniec, *J. Phys. Chem. B*, 2000, **104**, 11465–11471.
161 M. Kruk, M. Jaroniec, C. H. Ko and R. Ryoo, *Chem. Mater.*, 2000, **12**, 1961–1968.
162 p. 374 in ref. 1.
163 D. A. Loy, G. M. Jamison, B. M. Baugher, E. M. Russick, R. A. Assink, S. Prabakar and K. J. Shea, *J. Non-Cryst. Solids*, 1995, **186**, 44–53.
164 D. W. Schaefer, G. Beaucage, D. A. Loy, K. J. Shea and J. S. Lin, *Chem. Mater.*, 2004, **16**, 1402–1410.
165 S. S. Prakash, C. J. Brinker, A. J. Hurd and S. M. Rao, *Nature*, 1995, **374**, 439–443.
166 K. Kanamori, Y. Kodera, G. Hayase, K. Nakanishi and T. Hanada, submitted.
167 Chapter 3 in ref. 1.
168 N. Hüsing, D. Brandhuber and P. Kaiser, *J. Sol-Gel Sci. Technol.*, 2006, **40**, 131–139.
169 S. Hartmann, D. Brandhuber and N. Hüsing, *Acc. Chem. Res.*, 2007, **40**, 885–894.

 This journal is © The Royal Society of Chemistry 2011